Pergamon

Geochimica et Cosmochimica Acta, Vol. 68, No. 19, pp. 3827-3843, 2004

0016-7037/04 $30.00 + .00

doi:10.1016/j.gca.2004.03.009

New constraints on the sources and behavior of neodymium and hafnium in seawater from Pacific Ocean ferromanganese crusts

Tina van de Flierdt,[1,2,*] Martin Frank,[2] Der-Chuen Lee,[2,3] Alex N. Halliday,[2] Ben C. Reynolds,[2] and James R. Hein[4]

[1]Lamont-Doherty Earth Observatory of Columbia University, 61 Route 9W, Palisades, NY 10964, USA
[2]Institute for Isotope Geology and Mineral Resources, ETH-Zentrum, Sonneggstrasse 5, CH-8092 Zürich, Switzerland
[3]Institute of Earth Sciences, Academia Sinica, 128 Academia Road Sec. 2, Nankang, Taipei 115, Taiwan, ROC
[4]U.S. Geological Survey, 345 Middlefield Road, MS-999, Menlo Park, CA 94025, USA

(Received June 6, 2003; accepted in revised form March 2, 2004)

Abstract—The behavior of dissolved Hf in the marine environment is not well understood due to the lack of direct seawater measurements of Hf isotopes and the limited number of Hf isotope time-series obtained from ferromanganese crusts. In order to place better constraints on input sources and develop further applications, a combined Nd-Hf isotope time-series study of five Pacific ferromanganese crusts was carried out. The samples cover the past 38 Myr and their locations range from sites at the margin of the ocean to remote areas, sites from previously unstudied North and South Pacific areas, and water depths corresponding to deep and bottom waters.

For most of the samples a broad coupling of Nd and Hf isotopes is observed. In the Equatorial Pacific ε_{Nd} and ε_{Hf} both decrease with water depth. Similarly, ε_{Nd} and ε_{Hf} both increase from the South to the North Pacific. These data indicate that the Hf isotopic composition is, in general terms, a suitable tracer for ocean circulation, since inflow and progressive admixture of bottom water is clearly identifiable.

The time-series data indicate that inputs and outputs have been balanced throughout much of the late Cenozoic. A simple box model can constrain the relative importance of potential input sources to the North Pacific. Assuming steady state, the model implies significant contributions of radiogenic Nd and Hf from young circum-Pacific arcs and a subordinate role of dust inputs from the Asian continent for the dissolved Nd and Hf budget of the North Pacific.

Some changes in ocean circulation that are clearly recognizable in Nd isotopes do not appear to be reflected by Hf isotopic compositions. At two locations within the Pacific Ocean a decoupling of Nd and Hf isotopes is found, indicating limited potential for Hf isotopes as a stand-alone oceanographic tracer and providing evidence of additional local processes that govern the Hf isotopic composition of deep water masses. In the case of the Southwest Pacific there is evidence that decoupling may have been the result of changes in weathering style related to the buildup of Antarctic glaciation.

1. INTRODUCTION

The application of Hf isotopes to low-temperature environmental processes was first explored in the mid 1980s by Patchett et al. (1984) and White et al. (1986). It took, however, almost another decade before the investigation of Hf isotopes in the marine realm was taken up again (Godfrey et al. 1997; Albarède et al. 1998; Lee et al., 1999; Vervoort et al., 1999; Piotrowski et al., 2000; David et al., 2001; Pettke et al., 2002b; van de Flierdt et al., 2002). Despite rising interest in the behavior of hafnium in the sediment-seawater system, our present-day knowledge is relatively poor. This is mainly due to the fact that no direct analysis of Hf isotopes in seawater, river waters, or hydrothermal fluids are available, due to very low concentrations and related analytical difficulties. Thus, no detailed studies have been carried out to investigate the input pathways of Hf to the oceans. Recent analytical and technical progress facilitated by the development of multiple collector inductively coupled plasma mass spectrometry (MC-ICP-MS) suggest that such measurements will be feasible in the near future, but in the meantime records from other sources and archives have to be used to investigate the low-temperature geochemistry of hafnium.

The best constrained such archives are ferromanganese crusts. They permit reconstruction of the Hf isotopic composition of present and past seawater and enable the evaluation of potential input sources and supply mechanisms. Ferromanganese crusts are pristine seawater precipitates, which incorporate dissolved trace metals from the water column, most likely by coprecipitation with Fe and Mn oxides and oxyhydroxides (Koschinsky and Halbach, 1995). Based on studies of ferromanganese crusts (Godfrey et al., 1997; Lee et al., 1999; David et al., 2001) and analyses of Hf concentrations in the water column (McKelvey, 1994; Godfrey et al., 1996; McKelvey and Orians, 1998), the average residence time of Hf in seawater has been estimated to be on the order of 600–2000 yr. This is essentially the same as that of Nd (600–2000 yr; Jeandel, 1993; Jeandel et al., 1995; Tachikawa et al., 1999) and implies that Hf isotopes in seawater, like Nd isotopes, should provide information about ocean circulation patterns and/or input sources. If the residence time estimate for Hf is realistic, any advected Nd isotopic signature in the ocean should be coupled with a characteristic advected Hf isotopic signature. In turn, any observed decoupling of Nd and Hf isotopes in the ocean would point to (i) different input sources of the two trace metals and/or (ii)

* Author to whom correspondence should be addressed (tina@ldeo.columbia.edu).

different processes governing the Sm-Nd and Lu-Hf distribution in the sediment-seawater system.

Regarding input sources, early work by White et al. (1986) and subsequently by Godfrey et al. (1997) suggested that Hf from hydrothermal sources may play an important role for the dissolved Hf budget in the ocean. In contrast, it has been shown that the flux of hydrothermal Nd is negligible, because of very strong particulate scavenging of rare earth elements in and near vents (German et al., 1990; Halliday et al., 1992). A negligible hydrothermal Nd flux should result in a decoupling of Hf and Nd isotopes in seawater near hydrothermal vent sites. Some processes governing Sm-Nd and Lu-Hf systems in the sedimentary cycle have already been identified. In the crust-mantle system, Nd and Hf isotopes show a close coupling and form a well-defined "terrestrial array" when plotting Nd versus Hf isotopic composition (Vervoort et al., 1999). Ferromanganese crusts and nodules are archives of the seawater isotopic composition, and all data derived from these archives differ significantly from the terrestrial array for silicate rocks and define a separate and clearly defined array (the "seawater array"; Albarède et al., 1998). This offset has been attributed to the fact that the Lu-Hf system is subject to incongruent weathering effects on the continents leading to a preferential supply of radiogenic Hf to the ocean because most of the unradiogenic Hf contained in zircons is not released (e.g., Patchett et al., 1984; Vervoort et al., 1999). Such a process, in contrast, does not affect Nd isotopes in any significant way. Changes within the seawater array may therefore be used to trace changes in the style of weathering on the continents (Patchett et al., 1984; White et al., 1986; Albarède et al., 1998; Piotrowski et al., 2000; van de Flierdt et al., 2002).

To gain a better understanding of Hf-Nd isotope systematics in the ocean we have produced Hf and Nd isotope time-series data from 5 locations from the Pacific Ocean, ranging from 30°S to 50°N and from central to marginal oceanographic settings. With these data sets we almost triple the amount of Hf isotope records available for the Pacific Ocean, and increase the number of global records from 7 to 12. The recorded time intervals range from 7 to 38 Myr. We attempt to (i) place better constraints on the sources of Hf to the ocean over the Cenozoic, (ii) investigate the applicability of Hf as a circulation tracer, and (iii) establish further applications of Hf isotopes and combined Nd-Hf isotopes in the present and past marine environment.

2. SAMPLES AND METHODS

2.1. Samples and Dating Procedure

Five ferromanganese crusts from the Pacific Ocean were selected for analysis with the aim of adequately representing (i) different water depths, (ii) different latitudes, and (iii) remote as well as marginal oceanographic settings (Fig. 1). Details for each crust are given in Table 1. The age information on these crusts is published elsewhere (van de Flierdt et al., 2003, 2004a,b), and was obtained using a combined approach of $^{10}Be/^{9}Be$ dating for the younger parts ($\leq$10 Myr), and a Co-constant flux model for the older parts of the crusts. Major and trace element compositions for four of the five crusts show concentrations typical of a hydrogenous origin (van de Flierdt,

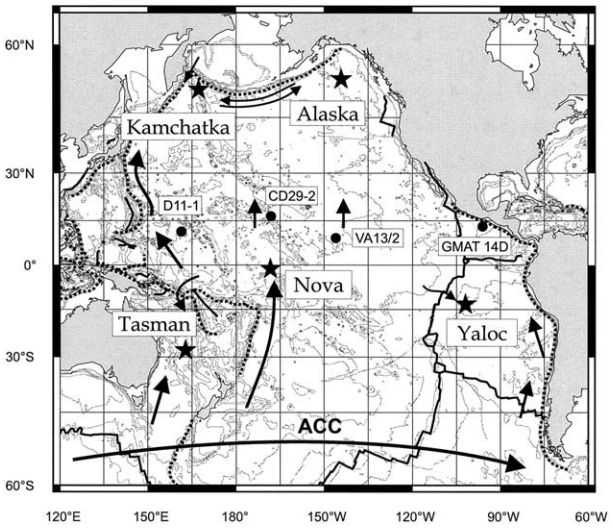

Fig. 1. Sample locations in the Pacific Ocean. Black arrows indicate schematically some of the main bottom water currents (ACC = Antarctic Circumpolar Current). Black lines delineate spreading centers and dotted lines delineate subduction zones. Black stars indicate the locations of our ferromanganese crusts and black circles indicate the locations of ferromanganese crusts studied previously.

2003). In crust Yaloc, however, the Fe and Cu contents rise with increasing age. This, together with unradiogenic Pb isotopes in the lower parts of the crust, points to a hydrothermal contribution (van de Flierdt et al., 2004b). Consequently, this crust is classified as mixed hydrogenetic-hydrothermal.

2.2. Hafnium Isotope Analysis

The crusts were sampled for Hf and Nd isotope analysis at a depth resolution of 2 to 10 mm corresponding to an age resolution between 0.4 and 4.3 Ma. Between 40 and 60 mg of material were used for each Hf isotope analysis. After sample dissolution for 30 to 90 min in a mixture of 6 M HCl and 2.5 M HF any residual material was removed by centrifugation (residue: $<$ 3% if present at all). The chemical separation of Hf followed the two-column procedure described by Lee et al. (1999). Separation of Lu from Hf was quantitative. However, due to high Yb concentrations in some samples, an improvement of the Yb-Hf separation was necessary, which was achieved by repeating the second ion-exchange column. Hafnium measurements were carried out on a Nu Plasma MC-ICP-MS at the ETH Zürich applying a $^{179}Hf/^{177}Hf$ ratio of 0.7325 to correct for instrumental mass fractionation. Tests with doped standard solutions showed that interferences from ^{176}Yb can be adequately corrected, if the ^{176}Yb contribution is less than $\sim$ 0.8% of the ^{176}Hf signal. The Yb contributions of all our samples were below that level. The long-term reproducibility was determined using a homogenized ferromanganese crust sample, which was processed several times independently through the column chemistry. Repeated analysis over a period of 10 months resulted in an external reproducibility of $\pm$ 0.48 ε units (2 σ standard deviation). As can be seen from Table 2a, some samples from crust Alaska did not reproduce that well. Most likely this was due to unresolved matrix problems of this

Table 1. Locations and details of crusts.[a]

Cruise, Sample Name	RNDB06, 13D-27A Kamchatka	S6-79-NP, D4-13A Alaska	SO36, 63KD Tasman	NovalX, D137-01 Nova	Yaloc73, D22-3 Yaloc
Location	NW Pacific	Gulf of Alaska	Lord Howe Rise	Central Pacific	Bauer Basin
Latitude	51°27.8′N	53°32.6′N	28°34.0′S	01°08.0′S	13°40.8′S
Longitude	167°38.2′E	144°22.4′W	163°00′E	168°04.0′W	102°08.1′W
Water Depth (m)	1800–1500	2100	1700	7129	4435–4212
Thickness (mm)	56	40	39	117.5	68
Dating/age model	(1)	(1)	(2)	(2)	(3)
Base Age (Ma)	9.9	3.6	23.3	38.1	7.2
Nd isotope data	this study	this study	(2)	(2)	(3)
Hf isotope data	this study	this study	this study	this study	(3)

[a] Sources of age models and isotope data other than this study: (1) van de Flierdt et al. (2003); (2) van de Flierdt et al. (2004a); and (3) van de Flierdt et al. (2004b).

particular crust given that all other samples were reproducible within the above quoted uncertainty. The larger uncertainties of these samples, however, do not affect any of our conclusions. Repeated analysis of the JMC475 Hf standard yielded a precision of 0.29–0.53 ε units on $^{176}Hf/^{177}Hf$ (2 σ standard deviation, derived from 8 measurement sessions, each consisting of 8 to 22 repeat analyses of the standard). All reported Hf isotope results in Table 2 were normalized to a $^{176}Hf/^{177}Hf$ ratio of 0.282160 for JMC475 (Nowell et al., 1998) to allow direct comparison with other published data. Measured JMC475 values are reported in Table 2. In the case of duplicate sample analyses, the average value is plotted in Figures 2–9.

2.3. Neodymium Isotope Analysis

Neodymium separation chemistry was performed on the fluorides precipitated in the initial step of the Hf chemistry. After converting the solution to Cl^- form, separation and purification was carried out as described by Cohen et al. (1988). Neodymium isotope measurements were also performed by MC-ICP-MS. To correct for instrumental mass bias $^{143}Nd/^{144}Nd$ ratios were normalized to $^{146}Nd/^{144}Nd$ of 0.7219. Repeated analysis of an in-house JMC Nd standard yielded a precision of 0.18–0.32 ε units on $^{143}Nd/^{144}Nd$ (2 σ standard deviation, derived from 8 measurement sessions, each consisting of 5 to 16 repeat analyses of the standard) over the period of the analysis of the 5 crusts (11 months). Precision of duplicate sample measurements on different days (same solutions) and for sample duplicates, which were processed independently through chemistry, was always within the external reproducibility of the standard measurements. To compare our in-house JMC values with the commonly used La Jolla standard several cross calibrations were carried out which gave a constant difference in $^{143}Nd/^{144}Nd$ of 0.000025 between the two standard solutions. $^{143}Nd/^{144}Nd$ ratios are reported relative to a JMC value of 0.511833, which corresponds to the nominal La Jolla value of 0.511858. In the case of duplicate sample analyses, the average value is plotted in Figures 2–9.

3. RESULTS

3.1. Alaska and Kamchatka (North Pacific)

Neodymium and Hf isotope time-series for crusts Alaska and Kamchatka (Fig. 1) are presented in Tables 2a and 2b and Figure 2a. Neodymium isotopes for the two North Pacific deep water sites exhibit very little variation (~ 1 ε unit) over the past 14 Myr and display similar average ε_{Nd} values in both crusts: -2.0 ± 0.5 (Alaska) and -2.2 ± 0.4 (Kamchatka) (Fig. 2a). The only resolvable feature in both profiles is a slight increase in ε_{Nd} from the time the crusts started to grow until 4.4 Ma (Alaska) and 5.1 Ma (Kamchatka), respectively, and a slight decrease in ε_{Nd} toward the surfaces of both crusts. These variations hardly exceed the analytical error. Comparison of direct deep water measurements from a nearby location (47°N, 161°E, 1795 m water depth, $\varepsilon_{Nd,\ corrected} = -3.2 \pm 0.5$; Piepgras and Jacobsen, 1988) with the surface of Kamchatka ($\varepsilon_{Nd} = -2.3 \pm 0.2$) shows a slight deviation from ambient deep water.

Hafnium isotopes are more variable over the two profiles and exhibit an overall range of $\varepsilon_{Hf} = 7.7$ to 9.8 (Kamchatka) and $\varepsilon_{Hf} = 6.5$ to 9.3 (Alaska) (Fig. 2a). The only trends outside analytical error are small decreases in ε_{Hf} starting at ~ 5.1 Ma in Kamchatka (contemporaneous with the decrease in ε_{Nd}) and at ~ 7.0 Ma in Alaska. Neodymium and Hf isotopes have obviously been coupled in their general trends, and—as expected—the range of the isotope data over the past 14 Myr is smaller for Nd than for Hf (1 ε unit compared to 2 ε units, respectively). Hafnium isotopic compositions for the surfaces are amongst the most radiogenic so far reported for ferromanganese crusts (Kamchatka: $\varepsilon_{Hf} = 8.0 \pm 0.4$; Alaska: $\varepsilon_{Hf} = 7.0 \pm 0.4$) and agree well with previously published data for the NW Pacific by Godfrey et al. (1997), when recalculated to the same standard and CHUR values.

3.2. Nova and Tasman (Southern Equatorial Pacific and Southwest Pacific)

Hafnium isotope time-series for crusts Tasman and Nova are presented in Table 2c and Figure 2b. Neodymium isotope data have been reported elsewhere (van de Flierdt et al., 2004a), but are also included in Figure 2b. The Hf isotope data of crust Nova are remarkably invariant showing no variation outside external reproducibility over the past 38 Myr ($\varepsilon_{Hf} = 5.7 \pm 0.4$). This contrasts with the Nd isotopes in the same crust, which show well-defined variations including a decrease of 1.6 ε units from 38 to 21 Ma and an increase in ε_{Nd} of 1.5 ε units toward present day. There is a clear decoupling of Nd and Hf isotope time-series in the deep Nova Canton Trough.

Table 2a. Nd and Hf isotope time-series for D4-13A (Alaska).

Depth interval (mm)	Age (Ma)	$^{176}Hf/^{177}Hf$[a] ± 2σ S.E.	ε_{Hf} (0)[b] ± 2σ S.D.	$^{143}Nd/^{144}Nd$[c] ± 2σ S.E.	ε_{Nd}(0)[d] ± 2σ S.D.
0–2	0.59	0.282964 ± 7	6.89 ± 0.33	0.512542 ± 10	−1.87 ± 0.24
duplicate*		0.282951 ± 8	6.44 ± 0.29		
duplicate**				0.512536 ± 7	−1.98 ± 0.23
duplicate*				0.512525 ± 11	−2.21 ± 0.32
0–2*		0.282973 ± 14	7.22 ± 0.52		
duplicate		0.282975 ± 12	7.29 ± 0.52		
2–4	1.78	0.283006 ± 7	8.39 ± 0.52	0.512550 ± 11	−1.72 ± 0.24
duplicate**				0.512536 ± 7	−1.98 ± 0.23
duplicate*				0.512534 ± 9	−2.04 ± 0.23
4–6	2.96	0.282989 ± 15	7.78 ± 0.53	0.512553 ± 14	−1.66 ± 0.28
duplicate**				0.512546 ± 10	−1.80 ± 0.23
4–6*		0.283000 ± 15	8.16 ± 0.53		
6–8	3.75	0.283008 ± 7	8.46 ± 0.33	0.512553 ± 5	−1.66 ± 0.24
duplicate*		0.282987 ± 13	7.72 ± 0.46		
8–10	4.40	0.282975 ± 9	7.30 ± 0.33	0.512555 ± 7	−1.62 ± 0.24
duplicate*				0.512558 ± 11	−1.57 ± 0.24
8–10*		0.283012 ± 11	8.60 ± 0.52		
10–12	5.06	0.282986 ± 12	7.69 ± 0.42	0.512543 ± 8	−1.85 ± 0.24
12–14	5.71	0.282996 ± 8	8.03 ± 0.33	0.512528 ± 7	−2.15 ± 0.24
duplicate**				0.512549 ± 10	−1.74 ± 0.23
14–16	6.37	0.283022 ± 10	8.96 ± 0.35	0.512541 ± 8	−1.90 ± 0.24
duplicate*				0.512554 ± 19	−1.64 ± 0.38
duplicate***		0.283021 ± 21	8.90 ± 0.74		
16–18	7.02	0.283034 ± 13	9.37 ± 0.46	0.512528 ± 8	−2.15 ± 0.24
duplicate*				0.512549 ± 8	−1.73 ± 0.24
18–20	7.68	0.283025 ± 7	9.05 ± 0.33	0.512525 ± 7	−2.21 ± 0.24
18–20*		0.283023 ± 8	9.00 ± 0.52		
20–22	8.34	0.283015 ± 8	8.69 ± 0.33	0.512544 ± 10	−1.83 ± 0.24
duplicate**				0.512521 ± 8	−2.29 ± 0.23
duplicate*				0.512515 ± 8	−2.40 ± 0.32
22–24	8.99	0.283001 ± 9	8.21 ± 0.33	0.512537 ± 12	−1.96 ± 0.24
duplicate*		0.283034 ± 20	9.36 ± 0.71		
24–26	9.65	0.282972 ± 6	7.19 ± 0.33	0.512516 ± 12	−2.38 ± 0.24
duplicate*		0.282953 ± 13	6.50 ± 0.46	0.512530 ± 11	−2.10 ± 0.24
24–26*		0.282998 ± 12	8.09 ± 0.52		
26–28	10.15	0.282996 ± 6	8.03 ± 0.33	0.512525 ± 7	−2.21 ± 0.24
duplicate*		0.282955 ± 10	6.57 ± 0.35		
28–30	10.63	0.283001 ± 11	8.21 ± 0.39	0.512505 ± 9	−2.60 ± 0.24
duplicate**				0.512507 ± 9	−2.55 ± 0.23
duplicate***		0.283023 ± 14	8.98 ± 0.50		
30–33	11.35	0.282971 ± 10	7.14 ± 0.35	0.512504 ± 7	−2.62 ± 0.24
duplicate***		0.282926 ± 16	5.55 ± 0.57		
30–33*		0.282999 ± 11	8.15 ± 0.52		
33–36	12.21	0.282954 ± 19	6.53 ± 0.67	0.512508 ± 14	−2.54 ± 0.28
33–36*		0.282987 ± 9	7.70 ± 0.52		
36–40	13.13	0.283006 ± 11	8.39 ± 0.39	0.512522 ± 18	−2.26 ± 0.35
duplicate**				0.512511 ± 13	−2.48 ± 0.23
36–40*		0.283004 ± 17	8.32 ± 0.60		

Duplicate* = same solution; duplicate** = same sample powder, independently run through chemistry; duplicate*** = original solution got processed a second time through chemistry; 0–2* = depth interval was newly sampled.

[a] For compatibility all ratios were normalized to a JMC475 value of 0.282160; given errors represent 2σ standard errors of individual measurements; actually measured JMC475 values on 4 different measuring days in the course of 3 month were 0.282138 ± 9 (2σ s.d.; n = 15), 0.282133 ± 8 (2σ s.d.; n = 12), 0.282134 ± 15 (2σ s.d.; n = 8), and 0.282134 ± 15 (2σ s.d.; n = 22).

[b] Calculated with $^{176}Hf/^{177}Hf_{CHUR}$ = 0.282769 (Nowell et al., 1998); errors for ε_{Hf} are reported as 2σ standard deviations resulting from repeated analysis of the JMC475 standard in the course of the sample measurements; in cases where the internal error is larger than the external one, the internal error is reported.

[c] For compatibility all ratios were normalized to a nominal La Jolla value of 0.511858; for further details see chapter 2; given errors represent 2σ standard errors of individual measurements; actually measured JMC values on 3 different measuring days in the course of 3 month were 0.511800 ± 12 (2σ s.d.; n = 16), 0.511795 ± 12 (2σ s.d.; n = 5), and 0.511821 ± 16 (2σ s.d.; n = 12).

[d] Calculated with $^{143}Nd/^{144}Nd_{CHUR}$ = 0.512638; errors for ε_{Nd} are reported as 2σ standard deviations resulting from repeated analysis of the JMC Nd standard in the course of the sample measurements; in cases where the internal error is larger than the external one, the internal error is reported.

The Hf isotopes in Southwest Pacific deep water (crust Tasman) show distinct trends with time. The time-series data display a progressive decrease in ε_{Hf} from 6.6 to 4.7 between 23 and 15 Ma, followed by a time interval of constant isotopic composition. From 10 Ma toward present day, a progressive trend toward higher values was recorded (overall increase of

Table 2b. Nd and Hf isotope time-series for 13D-27A (Kamchatka).

Depth interval (mm)	Age (Ma)	$^{176}Hf/^{177}Hf$[a] ± 2σ S.E.	ε_{Hf} (0)[b] ± 2σ S.D.	$^{143}Nd/^{144}Nd$[c] ± 2σ S.E.	ε_{Nd}(0)[d] ± 2σ S.D.
0–2	0.18	0.282992 ± 5	7.87 ± 0.52	0.512524 ± 5	−2.23 ± 0.18
duplicate		0.283001 ± 9	8.21 ± 0.41	0.512514 ± 8	−2.41 ± 0.22
4–6	0.88	0.282988 ± 8	7.73 ± 0.52	0.512529 ± 5	−2.13 ± 0.18
8–10	1.58	0.283009 ± 9	8.49 ± 0.52	0.512522 ± 6	−2.26 ± 0.18
duplicate		0.283012 ± 19	8.58 ± 0.68		
12–14.1	2.29	0.282995 ± 7	8.01 ± 0.52	0.512527 ± 6	−2.16 ± 0.18
16–18	2.99	0.283010 ± 6	8.53 ± 0.52	0.512529 ± 5	−2.13 ± 0.18
duplicate				0.512542 ± 12	−1.87 ± 0.23
20–22	3.70	0.283022 ± 9	8.95 ± 0.52	0.512542 ± 5	−1.88 ± 0.18
24–26	4.40	0.283018 ± 5	8.79 ± 0.52	0.512544 ± 9	−1.83 ± 0.18
28–30	5.11	0.283046 ± 8	9.79 ± 0.52	0.512547 ± 6	−1.77 ± 0.18
32–34	5.81	0.283036 ± 11	9.44 ± 0.52	0.512535 ± 8	−2.01 ± 0.18
36–38	6.51	0.283027 ± 8	9.14 ± 0.52	0.512533 ± 7	−2.04 ± 0.18
40–42	7.22	0.283032 ± 10	9.29 ± 0.52	0.512522 ± 20	−2.27 ± 0.40
44–46	7.92	0.283034 ± 9	9.39 ± 0.52	0.512520 ± 6	−2.30 ± 0.18
duplicate				0.512512 ± 9	−2.46 ± 0.22
48–52	8.80	0.283015 ± 8	8.72 ± 0.52	0.512505 ± 8	−2.60 ± 0.18
duplicate		0.283014 ± 7	8.65 ± 0.41	0.512503 ± 10	−2.63 ± 0.22
52–56	9.51	0.283046 ± 12	9.80 ± 0.52	0.512505 ± 7	−2.59 ± 0.18
duplicate		0.283029 ± 11	9.18 ± 0.41	0.512511 ± 14	−2.47 ± 0.27

[a] For compatibility all ratios were normalized to a JMC475 value of 0.282160; given errors represent 2σ standard errors of individual measurements; actually measured JMC475 values on 2 different measuring days were 0.282134 ± 15 (2σ s.d.; n = 22) and 0.282108 ± 12 (2σ s.d.; n = 10).

[b] Calculated with $^{176}Hf/^{177}Hf_{CHUR}$ = 0.282769 (Nowell et al., 1998); errors for ε_{Hf} are reported as 2σ standard deviations resulting from repeated analysis of the JMC475 standard in the course of the sample measurements; in cases where the internal error is larger than the external one, the internal error is reported.

[c] For compatibility all ratios were normalized to a nominal La Jolla value of 0.511858. Given errors represent 2σ standard errors of individual measurements; actually measured JMC values on 2 different measuring days were 0.511805 ± 9 (2σ s.d.; n = 11) and 0.511796 ± 11 (2σ s.d.; n = 6).

[d] Calculated with $^{143}Nd/^{144}Nd_{CHUR}$ = 0.512638; errors for ε_{Nd} are reported as 2σ standard deviations resulting from repeated analysis of the JMC Nd standard in the course of the sample measurements; in cases where the internal error is larger than the external one, the internal error is reported.

more than 2 ε units). These significant shifts in ε_{Hf} are only accompanied by a large shift in the Nd isotopic composition (2.4 ε units) for the time interval 10–0 Ma. This means that there was both a coupling (10–0 Ma) and a decoupling (23–15 Ma) of Nd and Hf isotopes at the same location.

3.3. Yaloc (Eastern Equatorial Pacific)

Neodymium and Hf isotope data for crust Yaloc from the eastern Equatorial Pacific (Bauer Basin) have been reported elsewhere (van de Flierdt et al., 2004b), but are shown in Figure 2c. Variations for both isotope systems hardly exceed the analytical error of the measurements over the past ~ 7 Myr. While Hf data scatter around an average value of ε_{Hf} = 6.6 ± 0.4, the Nd data show a slight upward trend of 0.7 ε units for the time interval from 5.8 to 2.9 Ma. The average ε_{Nd} value is −3.1 ± 0.3. Obviously, Nd and Hf isotopes have been coupled in that both systems do not show any major changes in the isotopic composition of ambient deep water over the growth period of the crust.

4. DISCUSSION

So far, the investigation of temporal changes in Nd and Hf isotopic compositions in the Pacific Ocean has been restricted to the equatorial area. Four Nd and three Hf isotope time-series have been reported: D11-1 (1800 m water depth; Ling et al., 1997; Lee et al., 1999; Figs. 1, 3, 5), CD29-2 (2300 m water depth; Ling et al., 1997; Lee et al., 1999; Figs. 1, 3, 5), VA13/2 (4830 m water depth; Abouchami et al., 1997; Ling et al., 1997; David et al., 2001; Figs. 1 and 4), and GMAT 14D (3400–4000 m water depth; Frank et al., 1999; Fig. 1). Out of the three records (D11-1, CD29-2, VA13/2) with both Nd and Hf isotope time-series, crusts D11-1 and CD29-2 show a pronounced decoupling throughout much of the Cenozoic as pointed out by Lee et al. (1999). This is in contrast to the data of VA13/2, which display a coupling of Hf and Nd isotopes at this location over the past 25 Myr (David et al., 2001). Consequently, it could be speculated that Nd and Hf isotopes have been coupled in bottom waters, but not in deep waters, since the water depth is the only significant difference between the three investigated locations.

Such speculation does not seem valid when incorporating our new record from crust Nova, that show a decoupling of Nd and Hf isotopes in Equatorial Pacific bottom waters (Figs. 4 and 5). Furthermore, a depth-related decoupling should also show up in the global data set of surface scrapings from ferromanganese crusts and nodules. However, Albarède et al. (1998) and David et al. (2001) observed exactly the opposite, which is a covariance of both isotope systems on a global scale. From all investigated Pacific time-series (this study and published data) it looks like (de)coupling of Nd and Hf isotopes is also not a simple function of geographic position. Both marginal sites and central sites do show coupling as well as decoupling (Figs. 1–5). In the following sections, we will first evaluate the influence of ocean circulation, input sources, and input mechanisms on the (coupled) Nd and Hf isotope records. Thereafter,

Table 2c. Hf isotope time-series for 63KD (Tasman) and D137-01 (Nova).

Depth interval (mm)	Age (Ma)	$^{176}Hf/^{177}Hf$[a] ± 2σ S.E.	ε_{Hf} (0)[b] ± 2σ S.D.
63KD (Tasman)			
0–1.5	0.39	0.282937 ± 10	5.93 ± 0.51
2–3	1.29	0.282970 ± 9	7.10 ± 0.51
4–5	2.32	0.282939 ± 8	6.01 ± 0.51
6–7	3.59	0.282953 ± 17	6.49 ± 0.61
9–10	6.56	0.282933 ± 11	5.81 ± 0.51
11–12	8.54	0.282928 ± 5	5.64 ± 0.51
13–14	10.23	0.282909 ± 7	4.95 ± 0.32
17–18	11.98	0.282912 ± 8	5.05 ± 0.32
20–21	13.61	0.282909 ± 7	4.94 ± 0.32
duplicate		0.282907 ± 11	4.90 ± 0.37
23–24	15.28	0.282898 ± 7	4.55 ± 0.32
duplicate		0.282903 ± 10	4.75 ± 0.34
27–28	17.84	0.282926 ± 5	5.54 ± 0.32
30–31	19.68	0.282926 ± 6	5.56 ± 0.32
34–35	21.40	0.282940 ± 9	6.03 ± 0.32
37–39	22.90	0.282955 ± 9	6.58 ± 0.32
D137-01 (Nova)			
0–1	0.11	0.282902 ± 14	4.69 ± 0.51
duplicate		0.282927 ± 16	5.59 ± 0.56
11–12	2.44	0.282914 ± 5	5.13 ± 0.32
21–23	4.67	0.282924 ± 4	5.48 ± 0.32
33–35	7.22	0.282940 ± 9	6.05 ± 0.32
duplicate		0.282925 ± 16	5.52 ± 0.56
45–47	9.82	0.282928 ± 7	5.61 ± 0.32
55–57	13.09	0.282933 ± 7	5.81 ± 0.32
65–67	16.77	0.282932 ± 7	5.75 ± 0.32
75–77	20.55	0.282920 ± 6	5.36 ± 0.32
duplicate		0.282946 ± 10	6.25 ± 0.36
85–87	24.86	0.282931 ± 7	5.74 ± 0.32
95–97	29.17	0.282934 ± 7	5.84 ± 0.32
105–107	33.34	0.282938 ± 5	5.96 ± 0.32
115–117.5	37.60	0.282936 ± 6	5.92 ± 0.32

[a] For compatibility all ratios were normalized to a JMC475 value of 0.282160; given errors represent 2σ standard errors of individual measurements; actually measured JMC475 values on 4 different measuring days in the course of one month were 0.282175 ± 14 (2σ s.d.; n = 32; two consecutive days), 0.282187 ± 9 (2σ s.d.; n = 17), and 0.282145 ± 10 (2s s.d.; n = 12).

[b] Calculated with $^{176}Hf/^{177}Hf_{CHUR}$ = 0.282769 (Nowell et al., 1998); errors for ε_{Hf} are reported as 2σ standard deviations resulting from repeated analysis of the JMC475 standard in the course of the sample measurements; in cases where the internal error is larger than the external one, the internal error is reported.

crusts Nova and Tasman, two local examples of decoupling, are discussed along with the published Equatorial Pacific records.

4.1. Neodymium-Hafnium Isotope Coupling in the Pacific Ocean

4.1.1. Water Mass Characteristics

Our new data permit the first comparison of the radiogenic isotope evolution of deep water masses in the Pacific Ocean from a perspective of latitudinal variability. The transport time for deep water from the Atlantic via the ACC to the North Pacific has been estimated to be roughly 1000 yr (e.g., Roemmich and McCallister, 1989; England, 1995). On the other hand, von Blanckenburg and Igel (1999) calculated that the entire Pacific's water is replenished every 1100 yr by import of Antarctic Bottom Water (AABW). This is on the order of the residence times of Hf and Nd, and consequently the isotopic composition of both elements should mirror the general pattern of water mass distribution.

Figure 3 shows a South (28°S) to North (53°N) section through the Pacific at 2000 m water depth covering the past 25 Myr (crusts Tasman, D11-1, CD29-2, Kamchatka, and Alaska); Figure 1 and Figure 4 show a South to North (27°S to 9°N) section at a water depth >4800 m. With the exception of the most recent parts of the South Pacific record, there is a pronounced general trend of the Nd becoming more radiogenic from South to North. This trend, which is consistent with the present-day Nd isotopic distribution measured directly on seawater samples (e.g., Piepgras and Wasserburg, 1982; Piepgras and Jacobsen, 1988), has obviously been a persistent feature over at least the past 14 Myr for the whole Pacific, and at least over the past 25 Myr for the South and Equatorial Pacific. Hafnium isotopes display similar trends with ε_{Hf} values increasing northwards (Figs. 3 and 4). Again, the South Pacific record (crust Tasman) shows more variation in its Hf isotopic composition, but also some similarity to Equatorial Pacific deep water. The Nd-Hf isotope behavior in this crust, as well as the remarkably constant record of Equatorial Pacific bottom water (~ 7000 m, crust Nova), will be discussed later in more detail. Note that the majority of data representing the ACC in Figure 4 are not derived from the Pacific sector of the Southern Ocean since no time-series data are available from this area (see Frank et al., 2002, for one exception). Therefore, Nd and Hf isotope time-series from the Southern Indian Ocean have been used (Piotrowski et al., 2000; Frank et al., 2002). Data from Ulfbeck et al. (2001) from the deep western boundary current (DWBC) in the South Pacific, however, indicate exactly the same invariable Nd isotopic composition over the past 10 Myr ($\varepsilon_{Nd} \sim -8$) and uniform ε_{Hf} values of +3.2 to +4.4.

The Nd and Hf isotope records of crust Yaloc are not included in Figures 3 and 4 since the Bauer Basin is not directly situated on the main pathway of the global thermohaline conveyor, and therefore is not expected to follow the general systematics outlined above (Figs. 1 and 2). The same holds for crusts GMAT 14D from the eastern equatorial Pacific (Fig. 1; Frank et al., 1999). The coupled and uniform Nd and Hf isotope time-series from crust Yaloc show similar values to Equatorial Pacific deep water and are discussed elsewhere in more detail (van de Flierdt et al., 2004b).

In summary, Nd isotopes have followed the expected pattern for deep and bottom water mixing: Southern Ocean waters entering the South Pacific carry a signature of $\varepsilon_{Nd} \sim -8$ to -9 (Piepgras and Wasserburg, 1980; Piepgras and Wasserburg, 1982; Albarède et al., 1997). On their way North along the DWBC, this signal gets gradually mixed and/or diluted with Pacific deep water, and therefore evolves toward more radiogenic values (Figs. 3 and 4). In the North Pacific and in the marginal Equatorial Pacific, the most radiogenic Nd isotopes are observed in the global ocean ($\varepsilon_{Nd} = -1.9$ to -2.4; this study and Frank et al., 1999). Since there is no deep water formation in the North Pacific (e.g., Warren, 1983), North Pacific deep water obtains its isotopic signature from a mixture of advected bottom water and more radiogenic local sources. The persistent vertical stratification of Nd isotopes in the Equatorial Pacific over the past 26 Myr corroborates the suitability of Nd isotopes as circulation tracer, since the stratification is

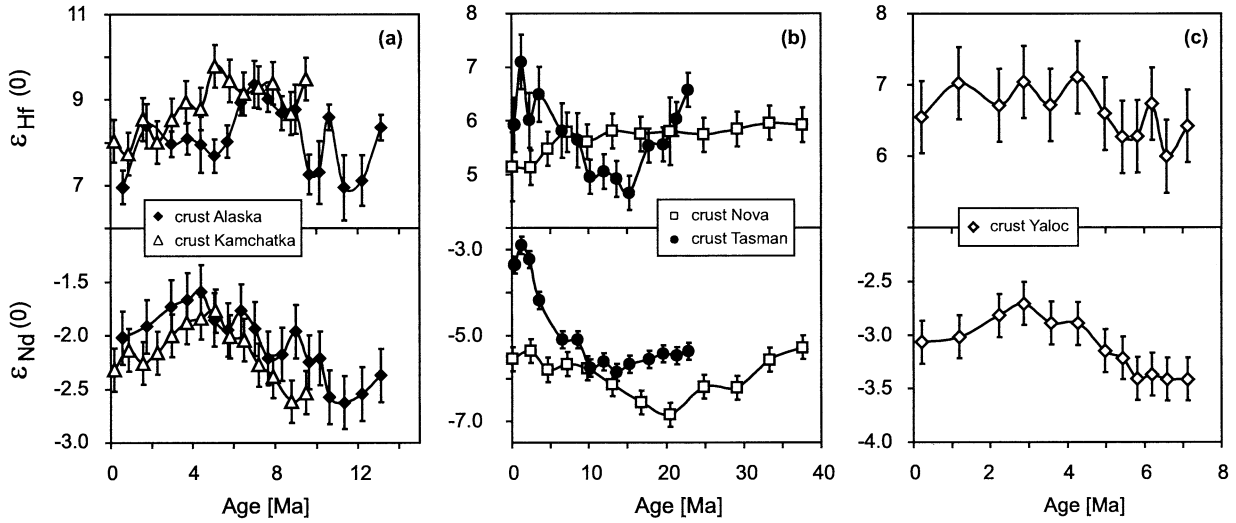

Fig. 2. Nd and Hf isotopes vs. age for the investigated ferromanganese crusts in this study. (a) Alaska (diamonds) and Kamchatka (open triangles), (b) Nova (open squares) and Tasman (circles), and (c) Yaloc (open diamonds). Note different scales on diagrams a–c. Data partly from van de Flierdt et al. (2004a,b).

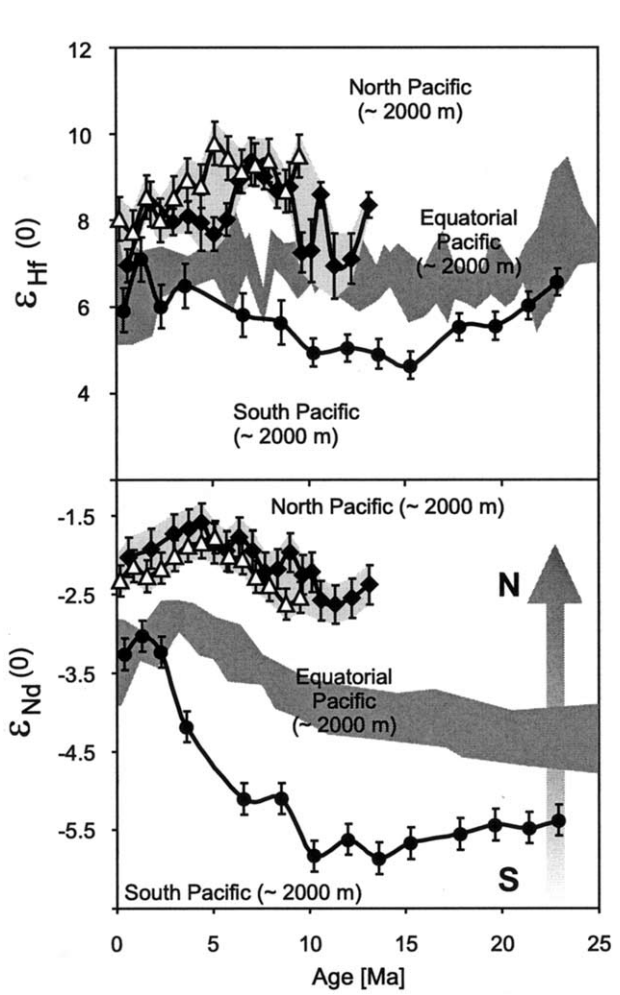

Fig. 3. Section through the Pacific at 2000 m water depth showing a persistent overall increase in ε_{Nd} and ε_{Hf} from the South to the North. North Pacific: crusts Alaska (diamonds) and Kamchatka (open triangles), Equatorial Pacific: crusts D11-1 and CD29-2 (data taken from Ling et al., 1997) South Pacific: crust Tasman (circles).

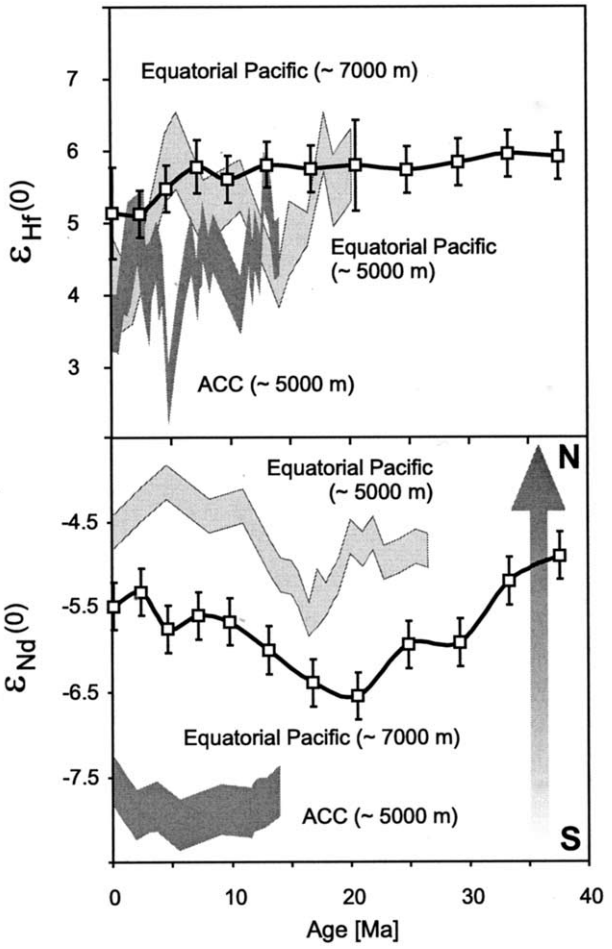

Fig. 4. South to North section from the Southern to Equatorial Pacific Ocean at water depths > 4800 m showing a persistent overall increase in ε_{Nd} and ε_{Hf} with decreasing latitude. ACC = Antarctic Circumpolar Current (data from Piotrowski et al., 2000; Frank et al., 2002), Equatorial Pacific, ~ 5000 m: crust VA13/2 (data from Ling et al., 1997; David et al., 2001), Equatorial Pacific, ~ 7000 m: crust Nova (open squares).

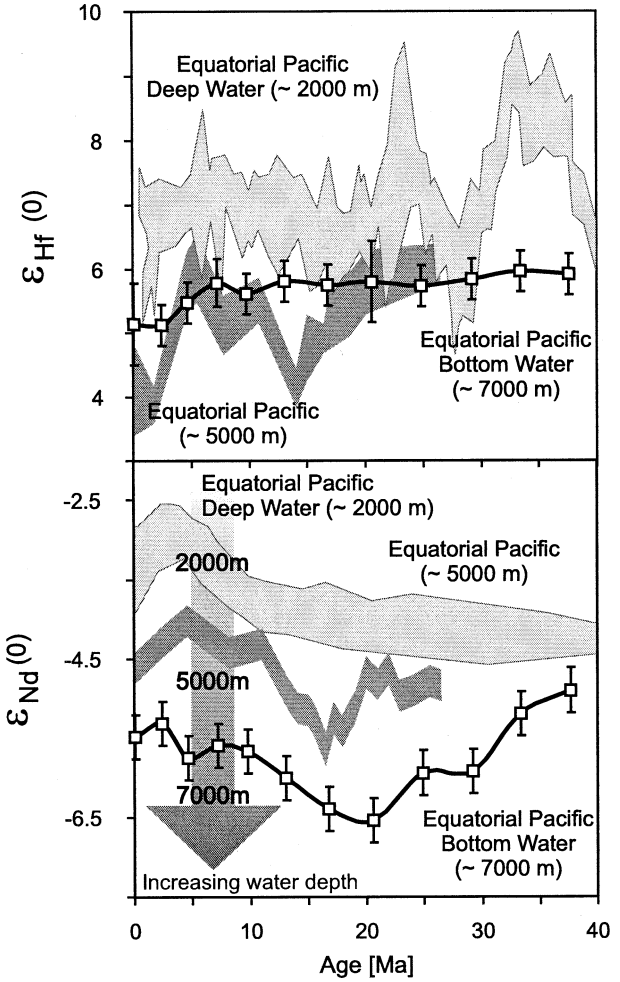

Fig. 5. Equatorial Pacific Nd and Hf isotope time-series, indicating a vertical stratification of the water column over the past at least 26 Myr. Data are derived from crusts D11-1 and CD29-2 (2000 m; Ling et al., 1997) crust VA13/2 (depth ~ 5000 m; Ling et al., 1997) and crust Nova (open squares).

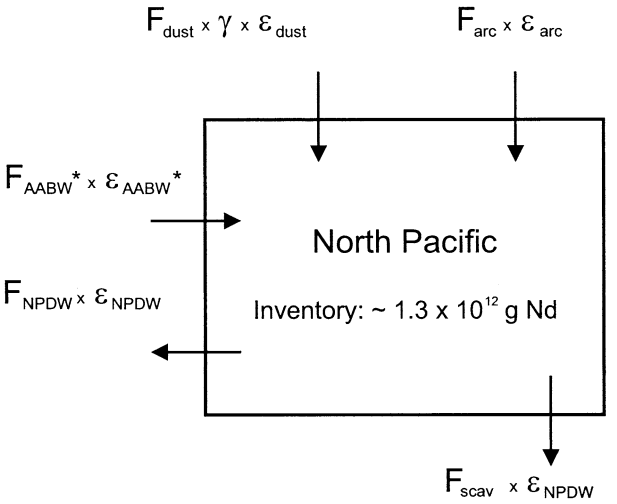

Fig. 6. Simple box model for the North Pacific, which assumes steady state, i.e., balanced fluxes and isotopic compositions, as described in the text. Abbreviations are defined in the text and in Table 3. The Nd inventory in the North Pacific is calculated with an area of the North Pacific of 9.4×10^7 km^2 (Uematsu et al., 2003), an average depth of 4 km, and an average Nd concentration of 3.5 ng/kg (see Alibo and Nozaki, 1999, and references in Table 3). In analogy an inventory of 4.0×10^{10} g is calculated for Hf, assuming an average Hf concentration of 0.1 ng/kg (McKelvey, 1994).

indicative of unradiogenic bottom water from the South (modified AABW) and more radiogenic, recirculated deep water from the North (NPDW) (Fig. 5; Ling et al., 1997).

Overall variations in the time-series data are smaller than latitudinal or vertical differences (Figs. 2–5) suggesting (i) that the overall present-day distribution of water masses in the Pacific Ocean has been similar back to Oligocene times, and (ii) that the residence times of Nd and Hf in the Pacific Ocean have not varied significantly over the past ~ 40 Myr. Since Hf isotopes show the same general trends as Nd isotopes, with the North Pacific being more radiogenic than the South Pacific (Figs. 3 and 4), and a vertical stratification of the water column (Fig. 5), it can be suggested that Hf isotope time-series can be used as a paleocirculation tracer as well. However, there are some restrictions. First, the Hf isotopes do not show profiles as smooth as those of Nd isotopes. This is mainly due to the larger analytical uncertainties involved and greater variability that leads to a larger overlap of records from different latitudes (e.g., North Pacific and Equatorial Pacific at 2000 m water depth or Southern Ocean and Equatorial Pacific at 5000 m water depth; Figs. 3 and 4). Second, two out of seven Pacific records in Figures 3, 4 and 5 do not show Hf isotope changes expected from water mass mixing only (crusts Nova and Tasman). Hence, we conclude that Hf isotopes are not as reliable as Nd isotopes as a stand-alone tracer for ocean circulation in the Pacific Ocean. Hafnium isotope records from ferromanganese crusts may support information on past ocean circulation, provided that they are coupled with Nd isotopes. On the other hand, and possibly more importantly, Hf isotopes may contain important information on other processes where decoupling from Nd isotopes is observed (section 4.2.).

4.1.2. Input Sources

Water masses entering the Pacific Ocean from the South have played an important role in governing the Nd and Hf isotopic composition of Pacific deep water (Abouchami et al., 1997; Ling et al., 1997; David et al., 2001). However, to balance the Nd and Hf isotopic composition of Pacific deep and bottom water (e.g., North Pacific deep water: $\varepsilon_{Nd} = -2.1$, $\varepsilon_{Hf} = +7.5$; crusts Alaska and Kamchatka), at least one end member is needed, which is significantly more radiogenic than advected AABW ($\varepsilon_{Nd} = -5.5$, $\varepsilon_{Hf} = +5.1$; crust Nova). The missing end member contains important information about external input sources of Nd and Hf to the Pacific Ocean. Neodymium and Hf isotopes in North Pacific deep water display parallel time-series patterns over the past 14 Myr (Fig. 3), and thus similar sources and input mechanisms for both isotope systems are likely. This observation excludes major contributions of hydrothermal Hf to North Pacific seawater, since the strong particulate scavenging of rare earth elements near vents (German et al., 1990; Halliday et al., 1992) does not permit a "hydrothermal" Nd isotope signature at this location. More

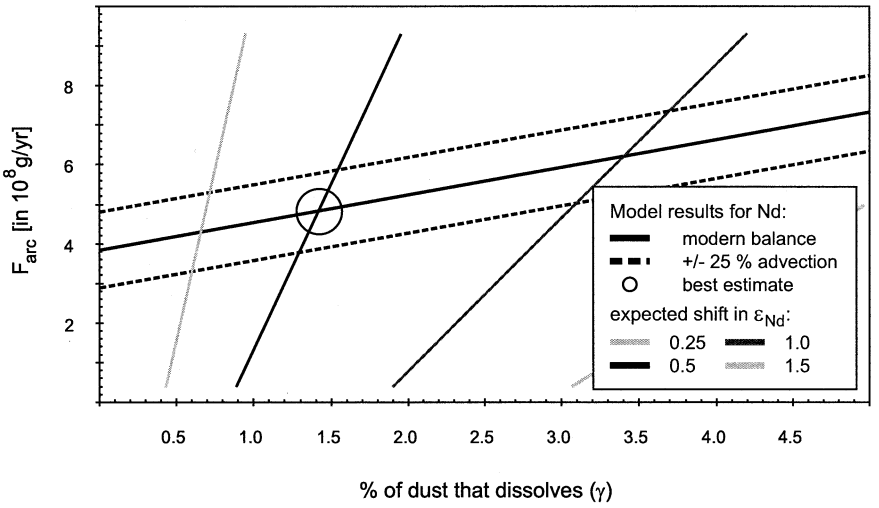

Fig. 7. Output data for the box model for the dust dissolution rate γ [%] and the arc flux F_{arc} [10^8 g/yr] to the North Pacific. Calculations are based on Eqns. 1 and 2 and data given for Nd in Table 3. The thick line represents the modern balance, and dashed lines indicate the shift in this balance if the advected Nd flux were to be 25% higher (or lower) than estimated in Table 3. Black and gray lines (almost vertical) represent model results for arc fluxes and dissolution rates, when subtracting Eqn. 2 at 3.5 Ma from Eqn. 2 at present day. The different lines monitor hypothetical shifts in the Nd isotopic composition of North Pacific deep water (0.25, 0.5, 1, and 1.5 ε units) due simply to the one order of magnitude increase in dust flux at 3.5 Ma, with other parameters staying constant. The circle highlights our best estimate on the dust dissolution rate γ and the arc flux, which is based on the modern balance and an observed shift in the Nd isotopic composition of North Pacific deep water of 0.5 ε units over the past 3.5 Ma (as seen in crusts Alaska and Kamchatka).

likely sources have been dust contributed to the North Pacific from the Asian continent and/or riverine inputs from the surrounding island arcs.

4.1.2.1. Asian Dust. Asian dust is characterized by a Nd isotopic composition of −10.3 (e.g., Pettke et al., 2000) and a Hf isotopic composition of $-4.7 < \varepsilon_{Hf} < +2.5$ (Pettke et al., 2002b). For both Nd and Hf, such values are distinctly less radiogenic than those of North Pacific deep waters. Therefore, large-scale leaching of continent-derived dust particles has obviously not been a suitable end member source to balance the Nd and Hf isotopic composition of the advected bottom waters to reach the values recorded by the North Pacific crusts. For Nd isotopes this has been concluded before by Nakai et al. (1993) and Jones et al. (1994), but has been questioned by for example Shimizu et al. (1994) on the basis of the Nd isotopic composition of a surface water sample from the central North Pacific. Pettke et al. (2002b) carried out the first study on the Hf isotopic composition of Asian dust and concluded that eolian dust was also not important for the Hf (and Nd; Pettke et al., 2002a) budget of the North Pacific before the one order of magnitude increase in dust flux to the North Pacific at ~3.5 Ma (see Rea, 1994). It is, however, possible that Hf and Nd released from dust particles had some effect on the seawater budget over the past 3.5 Myr since ferromanganese crust records from the Equatorial Pacific and the North Pacific (Fig. 3) show a slight decrease in Nd and Hf isotope ratios over exactly this time interval.

To evaluate the importance of Nd and Hf fluxes from different sources to the North Pacific, a simple box model was developed. Assuming steady state (i.e., a mass balance), a self-consistent model is presented, as detailed in Figure 6. The model is governed by two equations for (1) the balanced fluxes and (2) the balanced isotopic compositions, respectively, into and out of North Pacific seawater:

$$\gamma F_{dust} + F_{arc} + F_{AABW^*} = F_{scav} + F_{NPDW} \quad (1)$$

$$\gamma F_{dust}\varepsilon_{dust} + F_{arc}\varepsilon_{arc} + F_{AABW^*}\varepsilon_{AABW^*} = (F_{scav} + F_{NPDW})\varepsilon_{NPDW} \quad (2)$$

Abbreviations and symbols in Eqns. 1 and 2 are defined as follows:

γ: fraction of dust that is dissolved in the water column
F_{dust}: dust derived Nd (or Hf) flux to the North Pacific
ε_{dust}: Nd (or Hf) isotopic composition of the dust
F_{arc}: arc-derived Nd (or Hf) flux to the North Pacific
ε_{arc}: Nd (or Hf) isotopic composition of the arc end member
F_{AABW^*}: advected flux of Nd (or Hf) from modified AABW
ε_{AABW^*}: Nd (or Hf) isotopic composition of modified AABW
F_{scav}: flux of Nd (or Hf) scavenged out of the water column
F_{NPDW}: flux of Nd (or Hf) in deep water leaving the North Pacific
ε_{NPD^*}: Nd (or Hf) isotopic composition of NPDW

Most of the parameters in Eqns. 1 and 2, are fairly well constrained for Nd from results of this study and from the literature, but are more uncertain for Hf (Table 3). Hence, we will first introduce the model and its implications for Nd, and discuss constraints on the Hf fluxes in a separate paragraph at the end of this chapter.

Since no significant evaporation occurs, the water mass fluxes flowing into and out of the North Pacific must be equal (e.g., Schmitz, 1995). Given that the concentrations of Nd in

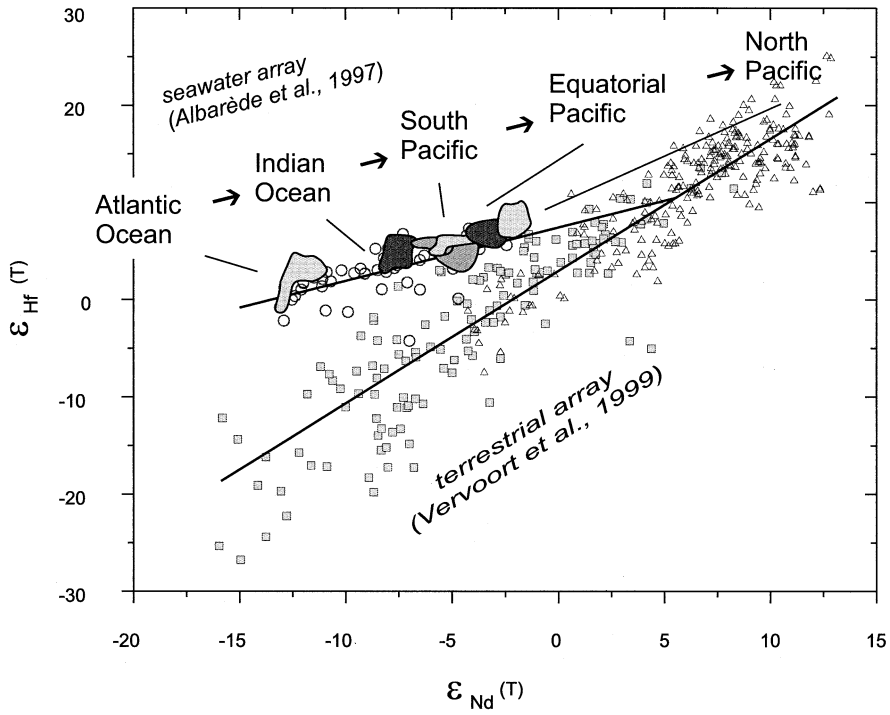

Fig. 8. Diagram of ε_{Nd} vs. ε_{Hf} showing the terrestrial array, the seawater array and fields for all ferromanganese time-series analyzed so far. The two North Pacific time-series from crusts Kamchatka and Alaska have been combined in one field. All time-series data plot along the seawater array. The least radiogenic data are found in the Atlantic Ocean, intermediate data in the Indian Ocean and the South Pacific, and North Pacific ferromanganese crusts display the most radiogenic data. This observation is consistent with the fact that Nd and Hf isotopes from ferromanganese crusts not only mirror the global conveyor belt, but also the composition of source terrains and incongruent weathering effects. The incongruent weathering effect for the Hf isotope system is most pronounced in the Atlantic Ocean due to the supply of Hf from old source terrains containing old zircons. Hence North Atlantic deep water exhibits the largest offset from the terrestrial array. The incongruent weathering effect is smallest in the North Pacific, where Nd and Hf are mainly derived from young, almost zircon-free source terrains. Gray triangles: mantle rocks; gray squares: crustal rocks; gray circles: ferromanganese crust surface scrapings.

NPDW and modified AABW (AABW*) are also roughly equal (see German et al., 1995, and references in Table 3), the total advected fluxes of Nd carried by NPDW and AABW* can be considered to be similar (Table 3). Hence, from Eqn. 1 the unknown output flux of Nd scavenged from the water column in the North Pacific (F_{scav}), can be defined as the sum of dust-derived dissolved Nd flux (γF_{dust}) and arc-derived dissolved Nd flux (F_{arc}) to the North Pacific. A more realistic multi-box model of a stratified water column with upwelling deep waters would not significantly alter this modeling assumption, because recirculating deep waters with higher concentrations would be balanced by surface water outflows with lower concentrations.

While the total dust-flux (F_{dust}) is reasonably well constrained through time from sediment mass accumulation rates in the central North Pacific (Table 3) estimates of the leachable/exchangeable fraction (γ) of Nd are highly variable (0–20%; Greaves et al., 1994; Tachikawa et al., 1999; Arraes-Mescoff et al., 2001). This dissolution parameter γ can be quite precisely constrained by our model for the North Pacific from the sensitivity of the deep water isotopic composition to the 10-fold increase in dust flux over the last 3.5 Myr. Assuming that the observed Nd isotopic change in NPDW (0.5 ε units; Fig. 3; Table 2), has only been a consequence of the change in the amount of dust delivered (i.e., island arc weathering, isotopic composition of dust, and water mass advection are kept constant), the dissolved flux of Nd originating from dust particles and from arc sources can be estimated. Clearly, the greater the amount of dust that dissolves in the water column, the more sensitive the budget will be to the 10-fold increase in dust flux. If, however, γ is chosen to be higher than a few percent, the increase in dust flux would have caused larger changes in the ε_{Nd} of NPDW (Fig. 7) than actually observed (Figs. 2 and 3). Since the recorded change in NPDW is less than 1 ε unit (including error bars on the Nd isotope measurements), the fraction of dust dissolving in the North Pacific cannot be greater than 3.4% and the total dust-derived Nd must have contributed less than 13% to the dissolved Nd budget of the North Pacific. Prior to the increase in dust deposition at 3.5 Ma the dust flux was 10 times smaller than at present day, and thus the effect of dissolved dust on the deep water composition must have been negligible for Nd. Even if the increase in dust deposition at 3.5 Ma had only been a factor of say 4, instead of 10, the modeled maximum dissolution rate of the dust would not become larger than 4.3%.

The combination of the new data in this study with available literature data facilitates narrow quantitative constraints on the importance of dust-derived contributions of Nd to the North

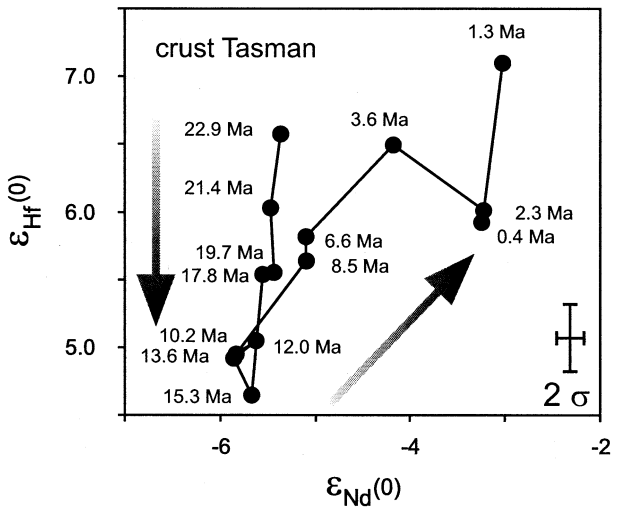

Fig. 9. Diagram of ε_{Nd} vs. ε_{Hf} for the time-series obtained for crust Tasman (Southwest Pacific Ocean). The vertical arrow indicates a trend resembling the one previously found in the North Atlantic (van de Flierdt et al., 2002), suggesting that the Hf isotopic composition of deep waters may have responded to the buildup of the East Antarctic Ice Sheet (see text). The second arrow represents a change in the Nd and Hf isotopic composition probably due to a change in ocean circulation induced by the closure of the Indonesian Gateway (van de Flierdt et al., 2004a). Numbers denote the age of each of the displayed samples.

Pacific. Despite the simplicity of the model its results are considered realistic because, forced by the new isotope results derived from the ferromanganese crusts, variations of the frame parameters within realistic ranges (Table 3) only lead to minor changes in the model results: For example, changing the flux of advected Nd by 50% results in a maximum shift in γ of 0.6%, and applying a Nd isotopic composition of -3 for NPDW (instead of -2) does not affect the modeled dust dissolution rate at all. Lowering the isotopic composition of ε_{Nd} from modified AABW toward an average value of -6.8 would only raise the maximal dissolution rate by 0.4% to a value of 3.8%. The only noticeable change in γ is observed, when choosing the two lowest possible values for calculating the dust flux ($[Nd]_{dust}$ = 26 ppm, Liu et al., 1993; mass accumulation rate of dust = 1.3×10^8 g/m^2/yr, Rea et al., 1998; Table 3), resulting in a maximal dust dissolution rates of 6.5%.

4.1.2.2. Arcs. As pointed out above, the box model also provides an estimate of the flux of arc-derived Nd. Assuming an average ε_{Nd} for the radiogenic arc-end member to be $+5$ (GEROC database, 2003; Table 3), the arc-derived flux of Nd (F_{arc}) cannot be less than 3.8×10^8 g/yr to meet the requirement to balance the isotopic composition of advected Nd (Fig. 7). Choosing, however, a lower Nd isotopic composition for the arc end member ($\varepsilon_{arc} = +2$) requires a higher F_{arc} of 8.9×10^8 g/yr, while an isotopic composition of $+10$ for the arc end member would result in a modeled arc-flux of 2.7×10^8 g/yr. Alteration of the applied isotopic composition of NPDW from -2 (derived from our crusts) to -3 (e.g., Piepgras and Jacobsen, 1988) would result in a slightly lower modeled arc flux of 3.3×10^8 g/yr. However, assuming also that our chosen isotopic composition for modified AABW may be slightly too high ($\varepsilon_{Nd} = -5.5$ instead of $\varepsilon_{Nd} = -6.8$, which represents the average of all published values; Table 3) the model results again in a higher arc flux of 4.8×10^8 g/yr.

Considering a suggested Nd inventory in the oceans of 5×10^{12} g (average value from estimates of Goldstein and Jacobsen, 1987, and Jeandel et al., 1995), and an average global residence time of Nd of 1000 yr (e.g., Tachikawa et al., 1999), a global Nd flux of 5×10^9 g/yr is calculated, which makes a flux of Nd above $\sim 10^9$ g/yr from the young volcanic arcs around the North Pacific alone unreasonably high (>20% of the global flux). Thus, to balance the isotopic budget with reasonable fluxes, the ε_{Nd} value of the arc source cannot have been less radiogenic than $+2$. Our preferred value is $+5$ as shown in Figure 7 and Table 3. Overall, the model supports significant contributions of Nd from very young basaltic terrains around the North Pacific and argues against large rivers as being the main contributor of Nd in this region.

There is support for this scenario from literature data for river systems. The Kurile-Kamchatka and Aleutian arc systems in the North Pacific have Nd isotopic compositions typically lying between $+5$ and $+10$ (GEOROC Database, 2003). It has previously been suggested that the average riverine discharge to the Pacific Ocean has a Nd isotopic composition of roughly -3 to -4 (Goldstein et al., 1984; Goldstein and Jacobsen, 1987). This estimate, however, was mainly based on the investigation of the very few large rivers entering the Pacific Ocean. Data for the dissolved load of smaller riverine systems draining young volcanic arcs are scarce but exhibit more radiogenic values (Mogami/Japan: $\varepsilon_{Nd} = 0.1$, four rivers from the Philippines: $\varepsilon_{Nd} = +6$ to $+7$; Goldstein and Jacobsen, 1987). By comparing these data with results for the suspended load from the same rivers, Goldstein and Jacobsen (1987, 1988) showed that dissolved and particulate loads yield similar Nd isotopic compositions in rivers draining young islands and continental arcs, and that these values are similar to the source rocks. In the light of this background information, it is reasonable to use the radiogenic signature of the rocks of the Aleutian and Kamchatkan arcs as end members for the evaluation of the Nd fluxes into the North Pacific.

4.1.2.3. Input Mechanisms from Arcs. There are two possible mechanisms for inputs of Nd from the arcs: (i) direct transport to the ocean via riverine pathways in dissolved form (e.g., Goldstein and Jacobsen, 1987; Elderfield et al., 1990), or (ii) release of Nd to seawater by exchange processes with particulate matter along the ocean margin ("boundary exchange"; Jeandel and Lacan, 2003; Tachikawa et al., 2003). The latter process includes both interaction of river particulates with seawater and near bottom dissolution of deposited or resuspended sediments at the continent/ocean interface (e.g., Spivack and Wasserburg, 1988; Bertram and Elderfield, 1993; Jeandel et al., 1995; Jeandel et al., 1998; Sholkovitz and Szymczak, 2000; Lacan and Jeandel, 2001; Tachikawa et al., 2003). At the present time none of the above listed possibilities can be excluded or quantified due to the lack of more detailed studies. This lack of other studies is why we have only identified the total dissolved/exchanged flux of Nd from the arcs (F_{arc}). The modeled value of 4.8×10^8 g/yr (Fig. 7) seems reasonable when compared to the study of Lacan and Jeandel (2001). These authors calculated a flux of 4.9×10^7 g Nd/yr being

Table 3. Input parameter for the North Pacific box model.

Parameter	Description	Estimated range for Nd (published data)	Modelled value for Nd	Reference	Estimated range for Hf (published data)	Modelled value for Hf	Reference
γ	Dissolution parameter	0 to 0.2	?	1–3	0 to 0.2	?	—
			Fluxes in 10^8 g/year				
F_{dust}	Present day dust flux	30 to 170	60[a]	4–11	2 to 50	11[a]	4–8, 12–13
F_{AABW*}	Advected flux into North Pacific	5 to 12	8[b]	14–19	—	0.2[b]	—
F_{NPDW}	Advected flux from North Pacific	4 to 18	8[c]	16–25	0.1 to 0.4	0.2[c]	16–19, 26–27
F_{arc}	Flux from arc material	—	?	—	—	?	—
F_{scav}	Scavenged flux	—	$F_{arc} + \gamma F_{dust}$	—	—	$F_{arc} + \gamma F_{dust}$	—
			Isotopic compositions in ε units				
ε_{dust}	of dust	−11.7 to −9.1	−10.3[d]	8, 10–11, 28–30	−4.7 to 2.5	−2.6[d]	13
ε_{AABW*}	of modified AABW	−8.1 to −5.4	−5.5[e]	14, 31–34	3.6 to 5.1	+5.1[e]	34–35
ε_{NPDW}	of NPDW	−6.8 to 0.0	−2.1[f]	14, 22–24, 33–34, 36–37	2.7 to 9.1	+7.5[f]	34–35, 38–40
ε_{arc}	of arc material	−16.4 to 11.8	+5.0[g]	41	12.0 to 18.0	+15.0[g]	42–43
ε_{scav}	Scavenged from North Pacific	−8.4 to 0.0	−2.1[h]	14, 22–24, 33, 36–37, 44–45	2.7 to 9.1	+7.5[h]	34–35, 38–40

Input parameter for North Pacific box model, with their estimated ranges from published data, and the values used in the described model. For modeling the isotopic mass balance at 3.5 Ma, the same input parameters have been chosen with two important modifications: (i) the dust flux is assumed to be lower by a factor of 10 (e.g. Rea et al., 1998) and (ii) the Nd and Hf isotopic composition of NPDW is lowered by 0.5 and 1 ε units respectively, as indicated by our time-series from crusts Alaska and Kamchatka (Figs. 2 and 3). For additional information, see main text.

References: 1, Greaves et al. (1994); 2, Tachikawa et al. (1999); 3, Arraes-Mescoff et al. (2001); 4, Duce et al. (1991); 5, Janecek and Rea (1983); 6, Rea et al. (1998); 7, Uematsu et al. (2003); 8, Taylor et al. (1983); 9, Liu et al. (1993); 10, Nakai et al. (1993); 11, Gallet et al. (1996); 12, Weber et al. (1996); 13, Pettke et al. (2002b); 14, Piepgras and Wasserburg (1982); 15, Nozaki and Alibo (2003); 16, Johnson and Toole (1993); 17, Roemmich & McCallister (1989); 18, Schmitz (1995); 19, Wijffels et al. (1996); 20, Alibo and Nozaki (1999); 21, Zhang et al. (1994); 22, Piepgras et al. (1979); 23, Piepgras and Jacobsen (1988); 24, Shimizu et al. (1994); 25, Piepgras and Jacobsen (1992); 26, McKelvey (1994); 27, McKelvey and Orians (1998); 28, Goldstein et al. (1984); 29, Liu et al. (1994); 30, Jones et al. (1994); 31, Albarède et al. (1997); 32, Amakawa et al. (1991); 33, Aplin et al. (1986); 34, Albarède et al. (1998); 35, White et al. (1986); 36, Goldstein and O'Nions (1981); 37, Ling et al. (1997); 38, Godfrey et al. (1997); 39, Lee et al. (1999); 40, David et al. (2001); 41, GEOROC database (2003); 42, White and Patchett (1984); 43, Münker et al. (2001); 44, O'Nions et al. (1978); 45, Elderfield et al. (1981).

[a] Modeled values are based on an area of the North Pacific of 9.4 $10^{13}m^2$ (Uematsu et al., 2002), a mass accumulation rate of dust of 2 $g/m^2/yr$ (Rea et al. 1998; Uematsu et al., 2002), and Nd and Hf concentrations in dust of 30 and 6 ppm, respectively (average of published data).

[b] Modeled values are based on advection of 7 Sverdrup (1 Sv = $10^6 m^3 s^{-1}$; e.g. Johnson and Toole, 1993) of modified AABW. Concentrations of Nd and Hf are assumed to be 3.5 ng/kg (Piepgras and Wasserburg, 1982; Nezaki and Alibo, 2003) and 0.1 ng/kg (no reference; value chosen in analogy to NPDW*).

[c] Modeled values are based on the same parameter as chosen for F_{AABW*} (e.g. Johnson and Toole, 1993; Alibo and Nozaki, 1999; McKelvey, 1994).

[d] Average of published data (e.g. Pettke et al., 2000; Pettke et al., 2002b).

[e] Values observed in this study from crusts Nova represent modified AABW (AABW*) at 1°S. Note that Nd and Hf isotopic compositions from crust Nova are at the high end of the published values for modified AABW in the South Pacific.

[f] Values obtained in this study from crusts Alaska and Kamchatka may only be representative for the marginal North Pacific and hence an alternative estimate for the Nd isotopic composition of NPDW over the entire North Pacific may be around −3 ε_{Nd} (e.g. Piepgras and Jacobsen, 1988).

[g] Average of published data. For ε_{Nd} some negative values from the Honshu arc have been excluded for determining the average.

[h] We assume that the isotopic composition of NPDW represents an appropriate average of the entire North Pacific water column (supported by the range of published data).

exchanged between the slope of Papua New Guinea and seawater. Note that our modeled value of 4.8×10^8 g/yr integrates the flux of Nd entering the North Pacific in dissolved form and the exchanged Nd. Furthermore, the area of slopes around the North Pacific is much larger compared to the Papua New Guinea area.

Since our calculated arc fluxes (2.7×10^8 to 8.9×10^8 g/yr assuming ε_{Nd} values between +10 and +2) are similar in magnitude to the estimated global dissolved riverine flux of Nd (5.0×10^8 g/yr; Goldstein and Jacobsen, 1987) a mass balance problem is indicated, which on a global scale has been called the "Nd paradox" (e.g., Bertram and Elderfield, 1993; Jeandel et al., 1995). The Nd paradox means that by applying literature estimates of the global riverine, and atmospheric fluxes of Nd

(Goldstein and Jacobsen, 1987; Duce et al., 1991; dust dissolution rate of 2%, Greaves et al., 1994; [Nd] = 30 ppm, Grousset et al., 1998), and the marine Nd inventory (Jeandel et al., 1995), a Nd residence time of ~ 5000 yr results. This is not realistic, since pronounced Nd isotopic differences are observed between water masses as well as a provinciality of Nd isotopes between different ocean basins (Fig. 8; see Piepgras et al., 1979; Goldstein and O'Nions, 1981). This provinciality provides strong evidence for a residence time for Nd not much longer than the global turnover time of the ocean of ~ 1500 yr (Broecker and Peng, 1982). The Nd isotopic provinciality is not only a present-day feature, but has been persistent over the entire Neogene, as can be seen from Figure 8 (Atlantic: ε_{Nd} = −13.1 to −10.5; Indian Ocean: ε_{Nd} = −8.1 to −7.0; Pacific Ocean: ε_{Nd} = −6.9 to −1.6; see also Frank, 2002, for a recent overview).

In general, an increase in the total Nd flux to the ocean is required to solve the Nd paradox, which can be achieved in three different ways: (i) increasing the dissolution rate of dust, (ii) increasing the supply of dissolved Nd to the ocean, or (iii) additional sources of Nd such as from particle/seawater exchange. The first possibility has been promoted by Tachikawa et al. (1999), who suggested that the soluble fraction of dust in seawater may be up to 20% in the eastern North Atlantic. Such a large amount of dust-derived Nd cannot be isotopically balanced in the case of the North Pacific (see section 4.1.2.1. and Fig. 7). The second suggestion, an increased supply of dissolved Nd, is supported by the work of Milliman and Syvitski (1992). It is quite possible that the role of small mountainous rivers has been severely underestimated, since the riverine Nd budgets have always been calculated based on the fluxes from large rivers alone. But large rivers have big estuaries, where a large fraction of the (dissolved) trace metals are removed (70% or even more; see Elderfield et al., 1990). Small mountainous rivers probably do not lose their dissolved load near the coast in this way since many of them discharge into the ocean at locations without large shelf areas. Even more likely is the possibility that exchange between particulates (river-borne or resuspended sediment) and seawater acts as an additional source. This is supported by Nd concentration profiles from the North Pacific, which exhibit a concentration maximum in deep to bottom waters and not in surface waters (e.g., Piepgras and Jacobsen, 1988). Furthermore, case studies from Papua New Guinea and the Indonesian Seas suggest that these "exchange processes" at the ocean margins are very important for governing the Nd isotopic composition of seawater (Jeandel et al., 1998; Sholkovitz et al., 1999; Amakawa et al., 2000; Sholkovitz and Szymczak, 2000; Lacan and Jeandel, 2001; see also Jones et al., 1994). One such process could for example be the release of trapped river water Nd in estuaries by increasing salinity (e.g., Sholkovitz and Szymczak, 2000). Moreover, a revisited calculation of the oceanic Nd budget using a steady state 10-box model and a compilation of field data by Tachikawa et al. (2003) suggests that Nd supply from continental margins can account for the missing Nd in the global budget. All the above cited studies imply that it is quite likely that the arcs around the Pacific Ocean, which have a very radiogenic Nd isotopic signature, are an essential source and end member for the global Nd budget, and may also contribute to solve the Nd paradox.

At this point, we would like to make a few remarks on the model results obtained for Hf by using the input parameters of the model defined in Table 3. Since the observed change in ε_{Hf} in North Pacific deep water has been less than 2 ε units over the past 3.5 Ma (Fig. 3), the fraction of dust dissolving in the North Pacific must be less than 1.1%, while the maximum contribution of dust to the Hf budget in the North Pacific is 22%. These model results have, however, to be treated with caution due to the lack of input data (Table 3). Moreover, we cannot assess at all how realistic the calculated arc flux of $\sim 0.12 \times 10^8$ g Hf/yr may be due to the unknown global Hf budget. As for Nd, the Hf input from dust seems to be negligible given our estimates of the model parameters (Table 3). Furthermore, the arc flux of Hf has obviously been very important, in agreement with the observed coupling of Nd and Hf isotopes in the North Pacific.

In summary, time-series of dissolved Nd and Hf isotopic composition in the Pacific Ocean reflect a long-term balance between eroded arc material on the one hand (radiogenic end member), and advected water masses (modified AABW) on the other. Eroded arc material is most likely supplied to the ocean by small rivers (dissolved load) and by exchange between seawater and arc-derived particulates. Dust dissolution has clearly been a source of subordinate importance for Nd and Hf in this region.

4.2. Neodymium-Hafnium Isotope Decoupling in the Pacific Ocean

On a global and basin-wide scale Nd and Hf isotopic compositions are coupled in ferromanganese crusts and monitor advection and mixing of water masses, as well as input from external sources. On a local scale, however, decoupling of Nd and Hf isotopes does occur. Every case of decoupling in a ferromanganese crust holds the potential to provide information about processes affecting the Hf isotopic composition of seawater. Two examples of decoupling of Nd and Hf isotope time-series from the Pacific Ocean are discussed below.

4.2.1. Glacial Weathering and the Hf Isotope Composition of Deep Water

Crust Tasman from the Lord Howe Rise in the Southwest Pacific Ocean (Fig. 1) displays both a coupling and decoupling of Nd and Hf isotopes within its 23 Myr record (Figs. 2 and 3). The large increase in the Nd isotopic composition over the past 10 Myr (2.8 ε units) can most likely be ascribed to a change in the circulation pattern in this area of the Pacific Ocean, and more specifically to the closure of the Indonesian Gateway (van de Flierdt et al., 2004a). The 2.8 ε unit change in Nd isotopes is accompanied by a 2.2 ε unit change in the Hf isotopic composition, pointing toward a similar origin for the Hf and Nd isotope changes. In analogy to the interpretation of the Nd isotope record, the pronounced shift in the Hf isotopic composition in the Southwest Pacific can be explained by mixing of two main water masses: Southern Ocean water (ε_{Hf} = +3 to +4; Ulfbeck et al., 2001) and Equatorial Pacific deep water (ε_{Hf} = +5.5 to +7.5 over the past 23 Ma; Lee et al., 1999), with the latter becoming progressively more important toward present day.

In addition, the Hf isotope pattern with time in crust Tasman

(Figs. 2 and 3) shows another significant change in the local deep water isotopic composition between 23 and 15 Ma. During this period, Hf isotopes decreased by ~ 2 ε units, whereas the Nd isotopic composition remained essentially constant. This Nd-Hf decoupling becomes even more obvious when the data are plotted in ε_{Nd} vs. ε_{Hf} space (Fig. 9): The data for the period 23 to 15 Ma show a coherent vertical trend toward lower ε_{Hf} values. In contrast, the ε_{Nd} and ε_{Hf} values during the past 10 Myr are correlated along a line, the slope of which is similar to the global seawater array (Fig. 8; Albarède et al., 1998). A vertical trend in ε_{Nd} vs. ε_{Hf} space has only been observed once before, namely in the Northwest Atlantic (Piotrowski et al., 2000; van de Flierdt et al., 2002). van de Flierdt et al. (2002) suggested that the Nd-Hf decoupling seen for the past 3 Myr in North Atlantic deep water was caused by release of highly unradiogenic Hf from very old zircons, facilitated by enhanced mechanical weathering during the onset of the Northern Hemisphere glaciation. They suggested that this process did not affect the Nd isotopic composition. Therefore the conclusion has been drawn that combined Nd-Hf isotope time-series studies may be a tool for assessing changes in the style of weathering in the geological past.

In the case of the Southwest Pacific, a similar explanation is reasonable, since the time interval from 23 to 15 Ma coincides with the buildup of the East Antarctic Ice Sheet (e.g., Billups and Schrag, 2002). Old cratonic rocks make up the continental basement in Antarctica, which were ground-up and eroded during these drastic environmental changes. For this reason, it is likely that some of the unradiogenic Hf, previously locked in the zircons, was released and exported to the Southern Pacific Ocean. This export led to a lowering in the Hf isotopic composition of Southwest Pacific deep water without being reflected in the Nd isotopic composition.

One way to check the reliability of the conclusions drawn above, is by comparing the Tasman record with other records situated under the direct influence of inflowing Southern Ocean water. Such records are crust Nova, from the Nova Canton Trough (Fig. 1) and crust 109D-C from the Southern Indian Ocean (27°58.4′S, 60°47.7 E; 5200–5700 m water depth; Piotrowski et al., 2000). None of these two crusts, however, shows a trend in their Hf isotopic compositions, similar to the one observed in Southwest Pacific. Hence it could be that crust Tasman is derived from a setting in which it mainly recorded the isotopic composition of waters, which formed nearby on the Antarctic continental shelf (e.g., Adelie coast; Rintoul et al., 2001). Although Pb and Nd isotope time-series from crust Tasman exclude any significant change in local input sources (van de Flierdt et al., 2004a), future studies are required to investigate potential other mechanisms that may be capable to change the Hf isotopic composition of seawater without affecting Nd and Pb isotopes.

4.2.2. *Behavior of Hafnium Isotopes in the Nova Canton Trough*

Crust Nova was recovered from a water depth of 7000 m in the Nova Canton Trough in the Southern Equatorial Pacific and reflects the composition of Equatorial Pacific bottom water. Although this location is directly at the outflow of the DWBC carrying modified AABW to the Equatorial Pacific (see Fig. 1), Hf isotopes from crust Nova present a puzzling picture: The Hf isotopic composition is more radiogenic than expected for water depth and latitude, and hardly any variability is visible for the past 38 Myr ($\varepsilon_{Hf} = 5.7 \pm 0.4$; Figs. 4 and 5). Constant Hf isotope data are in contrast to the variable Nd isotopic composition. Nd isotopes from crust Nova have been shown to be sensitive to changes in the import and composition of AABW over the past 38 Myr, due to the establishment of the ACC and the buildup of the East Antarctic Ice Sheet (Figs. 4 and 5; van de Flierdt et al., 2004a).

With the currently available data we cannot fully explain the Hf isotope behavior in crust Nova. We can, however, exclude some possibilities: First, it is clear that phosphatization did not erase or overprint the original signature, such as was speculated for other crusts from the Equatorial Pacific (Ling et al., 1997). This is manifested by P contents of less than 0.55% throughout crust Nova. Second, external sources (e.g., arcs) cannot be responsible for the elevated Hf isotopic composition, since any advected water mass showing an arc-like Hf isotopic signature would also show an arclike Nd isotopic signature (i.e., a coupling of Nd and Hf isotopes). Hydrothermal influence on the Hf profile can also be ruled out, due to typical hydrogenetic element concentrations in crust Nova (van de Flierdt, 2003; see also Hein et al., 2000). Third, differences in the speciation of Hf and Nd in seawater, as well as their partitioning into the oxyhydroxides of the ferromanganese crusts, could possibly result in different particle reactivity and hence residence times. Dissolved Hf in oxygenated seawater is present as neutral or negatively charged hydroxide complexes, which are associated and coprecipitated with the FeOOH phase of ferromanganese crusts (Bruland, 1983; Koschinsky and Hein, 2003). Neodymium, on the other hand, forms both positively charged monocarbonate complexes and negatively charged dicarbonate complexes. Most likely, the positively charged species is dominant, and is preferentially adsorbed onto MnO_2 phases. It is, however not obvious how this difference in chemical properties could cause the observed isotopic differences of the two elements.

We would like to point out that two out of the three published Equatorial Pacific ferromanganese crust time-series (D11-1 and CD29-2; Fig. 1) also shows a decoupling of Nd and Hf isotopes, at least over the past ~ 12 Myr (Figs. 3 and 5; Lee et al., 1999). While Nd isotopes have been shifted systematically toward more radiogenic values, there is no significant change in the Hf isotopic composition. Nevertheless, Nd and Hf isotopes in these two records appear to be correlated: Both isotope systems display the expected values in terms of the vertical stratification of the water column as well as in terms of their latitudinal position within Pacific deep water (Figs. 3 and 5; section 4.1.1.). Also deep crust VA13/2 (Figs. 1, 4, 5) fits the Pacific-wide distribution in terms of its Nd isotopic composition, but shows a coupling of Nd and Hf isotopes. Comparing, however, this deep Hf isotope record to our deep one of crust Nova, it is not clear which of the two records might be disturbed (Figs. 4 and 5). It is possible that the data do not indicate a decoupling of Nd and Hf isotopes in the Equatorial Pacific, but just reveal the fact that the Equatorial Pacific ferromanganese crusts have recorded the poorer sensitivity of the Hf isotope system to changes in water mass circulation compared to the Nd isotope system.

5. CONCLUSIONS

We presented a combined Nd-Hf time-series study of ferromanganese crusts from 5 locations in the Pacific Ocean, covering the past 38 Myr.

Consistent basin-wide patterns of Nd and Hf isotope time-series in the deep Pacific Ocean are a consequence of the general circulation pattern of northward advection of AABW and subsequent mixing with overlying Pacific deep water. This is documented by a pronounced and continuous latitudinal increase in the isotopic compositions of both systems in deep waters over at least the past 14 Myr. There also is clear evidence that a vertical stratification in the Equatorial Pacific water column has persisted over the past 25 Myr as a consequence of this circulation pattern, with less radiogenic values at depth. The fact that the overall variations within each of the Hf and Nd isotope time-series are smaller than latitudinal or vertical differences points to a long-term stable balance of Nd and Hf input sources to the Pacific Ocean. The two main factors controlling this balance have been: (i) advection of water masses from the Southern Ocean, and (ii) erosion and supply of Nd and Hf from young circum-Pacific island arcs. The importance of the latter (radiogenic) end member for the Nd and Hf isotopic composition of the North Pacific is corroborated by the results of a simple box model. The results from this model, along with the new data from this study, strongly support the view that island arcs have been a very important source in the global Nd and Hf budget. It is suggested that either small riverine systems, or exchange between particles and seawater at the ocean margins, or a combination of both, have been the main pathways for supplying arc-derived Nd and Hf to Pacific deep water. The simple box model also clearly demonstrates that dust must have been a minor component of the dissolved Nd and Hf budgets in the North Pacific, since calculated amounts of dust dissolution for Nd and Hf are less than 3.4% for both elements.

In general, the Nd and Hf isotope systems have been closely coupled in the Pacific Ocean at least during the past 14 Myr. There are, however, two examples from our data set and two examples from the literature, where this has not been the case. Although we are able to offer a possible interpretation for one of these cases, future studies are needed to better understand the mechanisms governing the Hf isotopic composition of seawater and its (de)coupling from Nd isotopes.

Acknowledgments—H. Baur, M. Meier, U. Menet, D. Niederer, F. Oberli, B. Rütsche, and A. Süsli are gratefully acknowledged for providing assistance with technical problems. M. Rehkämper, C. Stirling, H. Williams, and S. Woodland is thanked for keeping the machines running smoothly. Special thanks go to M. Rehkämper for advice in chemistry and mass spectrometry. We would like to acknowledge Andrea Koschinsky and Michael Bau for discussion about the deep water geochemistry of Nd and Hf, and J. Patchett for providing the JMC475 Hf standard solution. We thank A.M. Piotrowski and two anonymous reviewers for detailed comments. S.J.G. Galer is gratefully acknowledged for constructive suggestions, and for editorial handling. This research was funded by the Schweizerische Nationalfond (SNF).

Associate editor: S. J. G. Galer

REFERENCES

Abouchami W., Goldstein S. L., Galer S. J. G., Eisenhauer A., and Mangini A. (1997) Secular changes of lead and neodymium in central Pacific seawater recorded by a Fe-Mn crust. *Geochim. Cosmochim. Acta* **61**(18), 3957–3974.

Albarède F., Goldstein S. L., and Dautel D. (1997) The neodymium isotopic composition of manganese nodules from the Southern and Indian oceans, the global oceanic neodymium budget, and their bearing on deep ocean circulation. *Geochim. Cosmochim. Acta* **61**(6), 1277–1291.

Albarède F., Simonetti A., Vervoort J. D., Blichert-Toft J., and Abouchami W. (1998) A Hf-Nd isotopic correlation in ferromanganese nodules. *Geophys. Res. Lett.* **25,** 3895–3898.

Alibo D. S. and Nozaki Y. (1999) Rare earth elements in seawater: Particle association, shale-normalization, and Ce oxidation. *Geochim. Cosmochim. Acta* **63**(3/4), 363–372.

Amakawa H., Alibo D. S., and Nozaki Y. (2000) Nd isotopic composition and REE pattern in the surface waters of the eastern Indian Ocean and its adjacent seas. *Geochim. Cosmochim. Acta* **64**(10), 1715–1727.

Amakawa H., Ingri J., Masuda A., and Shimizu H. (1991) Isotopic compositions of Ce, Nd and Sr in ferromanganese nodules from the Pacific and Atlantic Oceans, the Baltic and Barents Seas, and the Gulf of Bothnia. *Earth Planet. Sci. Lett.* **105,** 554–565.

Aplin A., Michard A., and Albarède F. (1986) $^{143}Nd/^{144}Nd$ in Pacific ferromanganese encrustations and nodules. *Earth Planet. Sci. Lett.* **81,** 7–14.

Arraes-Mescoff R., Roy-Barman M., Coppola L., Souhaut M., Tachikawa K., Jeandel C., Sempéré R., and Yoro C. (2001) The behavior of Al, Mn, Ba, Sr, REE, and Th isotopes during in vitro degradation of large marine particles. *Mar. Chem.* **73,** 1–19.

Bertram C. J. and Elderfield H. (1993) The geochemical balance of the rare earth elements and neodymium isotopes in the oceans. *Geochim. Cosmochim. Acta* **57,** 1957–1986.

Billups K. and Schrag D. P. (2002) Paleotemperatures and ice volume of the past 27 Myr revisited with paired Mg/Ca and $^{18}O/^{16}O$ measurements on benthic foraminifera. *Paleoceanography* **17**(1), 10.1029/2000PA000567.

Broecker W. S. and Peng T.-H. (1982) *Tracers in the Sea.*Eldigio Press.

Bruland K. W. (1983) Trace Elements in Sea-water. In *Chemical Oceanography* (J. P. Riley, R. Chester), pp. 157–220. Academic Press.

Cohen A. S., O'Nions R. K., Siegenthaler R., and Griffin W. L. (1988) Chronology of the pressure-temperature history recorded by a granulite terrain. *Contrib. Mineral. Petrol.* **98,** 303–311.

David K., Frank M., O'Nions R. K., Belshaw N. S., Arden J. W., and Hein J. R. (2001) The Hf isotope composition of global seawater and the evolution of Hf isotopes in the deep Pacific Ocean from Fe-Mn crusts. *Chem. Geol.* **178,** 23–42.

Duce R. A., Liss P. S., Merrill J. T., Atlas E. L., Buat-Menard P., Hicks B. B., Miller J. M., Prospero J. M., Arimoto R., Church T. M., Ellis W., Galloway J. N., Hansen L., Jickells T. D., Knap A. H., Reinhardt K. H., Schneider B., Soudine A., Tokos J. J., Tsunogai S., Wollast R., and Zhou M. (1991) The atmospheric input of trace species to the world ocean. *Global Biogeochem. Cycles* **5**(3), 193–259.

Elderfield H., Hawkesworth C. J., and Greaves M. J. (1981) Rare earth element geochemistry oceanic ferromanganese nodules and associated sediments. *Geochim. Cosmochim. Acta* **45,** 513–528.

Elderfield H., Upstill-Goddard R., and Sholkovitz E. R. (1990) The rare earth elements in rivers, estuaries, and coastal seas and their significance to the composition of ocean waters. *Geochim. Cosmochim. Acta* **54,** 971–991.

England M. H. (1995) The age of water and ventilation timescales in a global ocean model. *J. Phys. Oceanogr.* **25,** 2756–2777.

Frank M. (2002) Radiogenic Isotopes. Tracers of past ocean circulation and erosional input. *Rev. Geophys.* **40**(1), 10.1029/2000RG000094.

Frank M., Reynolds B. C., and O'Nions R. K. (1999) Nd and Pb isotopes in Atlantic and Pacific water masses before and after closure of the Panama gateway. *Geology* **27,** 1147–1150.

Frank M., Whiteley N., Kasten S., Hein J. R., and O'Nions K. (2002) North. Atlantic deep water export to the Southern Ocean over the

past 14 Myr: Evidence from Nd and Pb isotopes in ferromanganese crusts. *Paleoceanography* **17**(2), 10.1029/2000PA000606.

Gallet S., Jahn B.-M., and Torii M. (1996) Geochemical characterization of the Luochuan loess-paleosol sequence, China, and paleoclimatic implication. *Chem. Geol.* **133,** 67–88.

GEOROC Database (2003) Geochemistry of rocks of the oceans and continents. MPI for Chemistry, Mainz, Germany. Available at: http://georoc.mpch-mainz.gwdg.de/.

German C. R., Klinkhammer G. P., Edmond J. M., Mitra A., and Elderfield H. (1990) Hydrothermal scavenging of rare-earth elements in the ocean. *Nature* **345,** 516–518.

German C. R., Masuzawa T., Greaves M. J., Elderfield H., and Edmond J. M. (1995) Dissolved rare earth elements in the Southern Ocean: Cerium oxidation and the influence of hydrography. *Geochim. Cosmochim. Acta* **59**(8), 1551–1558.

Godfrey L. V., White W. M., and Salters V. J. M. (1996) Dissolved zirconium and hafnium distributions across a shelf break in the northeastern Atlantic Ocean. *Geochim. Cosmochim. Acta* **60,** 3995–4006.

Godfrey L. V., Lee D.-C., Sangrey W. F., Halliday A. N., Salters V. J. M., Hein J. R., and White W. M. (1997) The Hf isotopic composition of ferromanganese nodules and crusts and hydrothermal manganese deposits: Implications for seawater Hf. *Earth Planet. Sci. Lett.* **151,** 91–105.

Goldstein S. J. and Jacobsen S. B. (1987) The Nd and Sr isotopic systematics of river-water dissolved material: Implications for the sources of Nd and Sr in seawater. *Chem. Geol.* **66,** 245–272.

Goldstein S. J. and Jacobsen S. B. (1988) Nd and Sr isotopic systematics of river water suspended material: Implications for crustal evolution. *Earth Planet. Sci. Lett.* **87,** 249–265.

Goldstein S. L. and O'Nions R. K. (1981) Nd and Sr isotopic relationships in pelagic clays and ferromanganese deposits. *Nature* **292,** 324–327.

Goldstein S. L., O'Nions R. K., and Hamilton P. J. (1984) A Sm-Nd isotopic study of atmospheric dusts and particulates from major river systems. *Earth Planet. Sci. Lett.* **70,** 221–236.

Greaves M. J., Statham P. J., and Elderfield H. (1994) Rare earth mobilization from marine atmospheric dust into seawater. *Mar. Chem.* **46,** 255–260.

Grousset F. E., Parra M., Bory A., Martinez P., Bertrand P., Shimmield G., and Ellan R. M. (1998) Saharan wind regimes traced by the Sr-Nd isotopic compositions of the subtropical Atlantic sediments: Last glacial maximum vs. today. *Quat. Sci. Rev.* **17,** 395–409.

Halliday A. N., Davidson J. P., Holden P., Owen R. M., and Olivarez A. M. (1992) Metalliferous sediments and the scavenging residence time of Nd near hydrothermal vents. *Geophys. Res. Lett.* **19,** 761–764.

Hein J. R., Koschinsky A., Bau M., Manheim F. T., Kang J.-K., and Roberts L. (2000) Cobalt-rich ferromanganese crusts in the Pacific. In *Handbook of Marine Mineral Deposits* (ed. D. S. Cronan). CRC Press, Boca Raton. pp. 239–279.

Janecek T. R. and Rea D. K. (1983) Eolian deposition in the northeast Pacific Ocean: Cenozoic history of atmospheric circulation. *Geol. Soc. Am. Bull.* **94,** 730–738.

Jeandel C. (1993) Concentration and isotopic composition of Nd in the South Atlantic Ocean. *Earth Planet. Sci. Lett.* **117,** 581–591.

Jeandel C. and Lacan F. (2003) Boundary processes traced by neodymium isotopes. *Geophys. Res. Abstr.* **5,** 08573.

Jeandel C., Bishop J. K., and Zindler A. (1995) Exchange of neodymium and its isotopes between seawater and small and large particles in the Sargasso Sea. *Geochim. Cosmochim. Acta* **59,** 535–547.

Jeandel C., Thouron D., and Fieux M. (1998) Concentrations and isotopic compositions of neodymium in the Indian Ocean and Indonesian Straits. *Geochim. Cosmochim. Acta* **62**(15), 2597–2607.

Johnson G. C. and Toole J. M. (1993) Flow of deep and bottom waters in the Pacific at 10°N. *Deep-Sea Res.* **40**(2), 371–394.

Jones C. E., Halliday A. N., Rea D. K., and Owen R. M. (1994) Neodymium isotopic variations in North Pacific modern silicate sediment and the insignificance of detrital REE contributions to seawater. *Earth Planet. Sci. Lett.* **127,** 55–66.

Koschinsky A. and Halbach P. (1995) Sequential leaching of marine ferromanganese precipitates: Genetic implications. *Geochim. Cosmochim. Acta* **59**(24), 5113–5132.

Koschinsky A. and Hein J. R. (2003) Uptake of elements from seawater by ferromanganese crusts: Solid phase associations and seawater speciation. *Mar. Geol.* **198**(3–4), 331–351.

Lacan F. and Jeandel C. (2001) Tracing Papua New Guinea imprint on the central Equatorial Pacific Ocean using neodymium isotopic compositions and rare earth element patterns. *Earth Planet. Sci. Lett.* **186,** 497–512.

Lee D.-C., Halliday A. N., Hein J. R., Burton K. W., Christensen J. N., and Günther D. (1999) Hafnium isotope stratigraphy of ferromanganese crusts. *Science* **285,** 1052–1054.

Ling H. F., Burton K. W., O'Nions R. K., Kamber B. S., von Blanckenburg F., Gibb A. J., and Hein J. R. (1997) Evolution of Nd and Pb isotopes in Central Pacific seawater from ferromanganese crusts. *Earth Planet. Sci. Lett.* **146,** 1–12.

Liu C.-Q., Masuda A., Okada A., Yabuki S., Zhang J., and Fan Z.-L. (1993) A geochemical study of loess and desert sand in northern China: Implications for continental crust weathering and composition. *Chem. Geol.* **106,** 359–374.

Liu C.-Q., Masuda A., Okada A., Yabuki S., and Fan Z.-L. (1994) Isotope geochemistry of Quaternary deposits from the arid lands in northern China. *Earth Planet. Sci. Lett.* **127,** 25–38.

McKelvey B. A. (1994) The marine geochemistry of Zr and Hf. Ph.D. thesis. University of British Columbia.

McKelvey B. A. and Orians K. J. (1998) The determination of dissolved zirconium and hafnium from seawater using isotope dilution inductively coupled plasma mass spectrometry. *Mar. Chem.* **60,** 245–255.

Milliman J. D. and Syvitski J. P. M. (1992) Geomorphic/tectonic control of sediment discharge to the ocean: The importance of small mountainous rivers. *J. Geol.* **100,** 525–544.

Münker C., Wörner G., Churikova T., and Mezger K. (2001) The HFSE budget of arc magmas: New models from Hf isotopes and isotope dilution measurements of Nb/Ta, Zr/Hf and Lu/Hf in Kamchatka arc rocks (abstract). *Eos* **82,** T31F–04.

Nakai S., Halliday A. N., and Rea D. K. (1993) Provenance of dust in the Pacific Ocean. *Earth Planet. Sci. Lett.* **119,** 143–157.

Nowell G. M., Kempton P. D., Noble S. R., Fitton J. G., Saunders A. D., Mahoney J. J., and Taylor R. N. (1998) High precision Hf isotope measurements of MORB and OIB by thermal ionisation mass spectrometry: Insights into the depleted mantle. *Chem. Geol.* **149,** 211–233.

Nozaki Y. and Alibo D. S. (2003) Dissolved rare earth elements in the Southern Ocean, southwest of Australia: Unique patterns compared to the South Atlantic data. *Geochem. J.* **37**(1), 47–62.

O'Nions R. K., Carter S. R., Cohen R. S., Evensen N. M., and Hamilton P. J. (1978) Pb, Nd and Sr isotopes in oceanic ferromanganese deposits and ocean floor basalts. *Nature* **273,** 435–438.

Patchett P. J., White W. M., Feldmann H., Kielinczuk S., and Hofmann A. W. (1984) Hafnium/rare earth element fractionation in the sedimentary system and crustal recycling into the Earth's mantle. *Earth Planet. Sci. Lett.* **69,** 365–378.

Pettke T., Halliday A. N., Hall C. M., and Rea D. K. (2000) Dust production and deposition in Asia and north Pacific Ocean over the past 12 Myr. *Earth Planet. Sci. Lett.* **178,** 397–413.

Pettke T., Halliday A. N., and Rea D. K. (2002a) Cenozoic evolution of Asian climate and sources of Pacific seawater Pb and Nd derived from eolian dust of sediment core LL44-GPC3. *Paleoceanography* **17,** 10.1029/2001PA000673.

Pettke T., Lee D.-C., Halliday A. N., and Rea D. K. (2002b) Radiogenic Hf isotopic compositions of continental eolian dust from Asia, its variability and its implications for seawater Hf. *Earth Planet. Sci. Lett.* **202,** 453–464.

Piepgras D. J. and Jacobsen S. B. (1988) The isotopic composition of neodymium in the North Pacific. *Geochim. Cosmochim. Acta* **52,** 1373–1381.

Piepgras D. J. and Jacobsen S. B. (1992) The behavior of rare earth elements in seawater: Precise determination of variations in the North Pacific water column. *Geochim. Cosmochim. Acta* **56,** 1851–1862.

Piepgras D. J. and Wasserburg G. J. (1980) Neodymium isotopic variations in seawater. *Earth Planet. Sci. Lett.* **50,** 128–138.

Piepgras D. J. and Wasserburg G. J. (1982) Isotopic composition of neodymium in waters from the Drake Passage. *Science* **217,** 207–214.

Piepgras D. J., Wasserburg G. J., and Dasch E. J. (1979) The isotopic composition of Nd in different ocean masses. *Earth Planet. Sci. Lett.* **45,** 223–236.

Piotrowski A. M., Lee D.-C., Christensen J. N., Burton K. W., Halliday A. N., Hein J. R., and Günther D. (2000) Changes in erosion and ocean circulation recorded in the Hf isotopic compositions of North Atlantic and Indian Ocean ferromanganese crusts. *Earth Planet. Sci. Lett.* **181,** 315–325.

Rea D. K. (1994) The paleoclimatic record provided by eolian deposition in the deep sea: The geologic history of wind. *Rev. Geophys.* **32**(2), 159–195.

Rea D. K., Snoeckx H., and Joseph L. H. (1998) Late Cenozoic eolian deposition in the North Pacific: Asian drying, Tibetan uplift, and cooling of the northern hemisphere. *Paleoceanography* **13**(3), 215–224.

Rintoul S. R., Hughes C. W., Olbers D. (2001) The Antarctic circumpolar current system. In *Ocean Circulation and Climate—Observing and Modelling the Global Ocean* (G. Siedler, J. Church, J. Gould) pp. 271–302. Academic Press.

Roemmich D. and McCallister T. (1989) Large scale circulation of the North Pacific Ocean. *Progr. Oceanogr.* **22,** 171–204.

Schmitz W. J.Jr. (1995) On the interbasin-scale thermohaline circulation. *Rev. Geophys.* **33**(2), 151–173.

Shimizu H., Tachikawa K., Masuda A., and Nozaki Y. (1994) Cerium and neodymium isotope ratios and REE patterns in seawater from the North Pacific Ocean. *Geochim. Cosmochim. Acta* **58,** 323–333.

Sholkovitz E. R. and Szymczak R. (2000) The estuarine chemistry of rare earth elements: Comparison of the Amazon, Fly, Sepik and the Gulf of Papua systems. *Earth Planet. Sci. Lett.* **179,** 299–309.

Sholkovitz E. R., Elderfield H., Szymczak R., and Casey K. (1999) Island weathering: River sources of rare earth elements to the Western Pacific Ocean. *Mar. Chem.* **68,** 39–57.

Spivack A. J. and Wasserburg G. J. (1988) Neodymium isotopic composition of the Mediterranean outflow and the eastern North Atlantic. *Geochim. Cosmochim. Acta* **52,** 2767–2773.

Tachikawa K., Jeandel C., and Roy-Barman M. (1999) A new approach to the Nd residence time in the ocean: The role of atmospheric inputs. *Earth Planet. Sci. Lett.* **170,** 433–446.

Tachikawa K., Athias V., and Jeandel C. (2003) Neodymium budget in the modern ocean and paleo-oceanographic implications. *J. Geophys. Res.*, **108**(C8),10.1029/1999JC0 00285.

Taylor S. R., McLennan S. M., and McCulloch M. T. (1983) Geochemistry of loess, continental crustal composition and crustal model ages. *Geochim. Cosmochim. Acta* **47,** 1897–1905.

Uematsu M., Wang Z., and Uno I. (2003) Atmospheric input of mineral dust to the western North Pacific region based on direct measurements and a regional chemical transport model. *Geophys. Res. Lett.* **30**(6), 10.1029/2002GL016645.

Ulfbeck D. G., Baker J. A., Graham I. J., and Wright I. C. (2001) Hf isotopic profiles of Fe-Mn nodules (19–0 Ma) from the deep western boundary current, southern Pacific (abstract). *Eos* **82,** OS31.C-0439.

van de Flierdt T., Frank M., Lee D.-C., and Halliday A. N. (2002) Glacial weathering and the hafnium isotope composition of seawater. *Earth Planet. Sci. Lett.***198**, 167–175. Republished with corrections: *Earth Planet. Sci. Lett.* **201,** 639–647.

van de Flierdt T. (2003) The Nd, Hf, and Pb isotopic composition of ferromanganese crusts and their paleoceanographic implications. Ph.D. thesis. ETH Zürich. Der Andere Verlas

van de Flierdt T., Frank M., Halliday A. N., Hein J. R., Hattendorf B., Günther D., and Kubik P. W. (2003) Lead isotopes in North Pacific deep water—Implications for past changes in input sources and circulation patterns. *Earth Planet. Sci. Lett.* **209,** 149–164.

van de Flierdt T., Frank M., Halliday A. N., Hein J. R., Hattendorf B., Günther D., and Kubik P. W. (2004a) Deep- and bottom-water export from the Southern Ocean to the Pacific over the past 38 million years. *Paleoceanography*, **19,** doi:10.1029/2003PA000923.

van de Flierdt T., Frank M., Lee D.-C., Halliday A.N. Hein.J.R., Hattendorf.B., Günther.D., Kubik.P.W.(2004) Tracing the history of submarine hydrothermal inputs using the Pb isotope composition of ferromanganese crusts . *Earth Planet. Sci. Lett.* **222,** 259–273.

Vervoort J. D., Patchett P. J., Blichert-Toft J., and Albarède F. (1999) Relationships between Lu-Hf and Sm-Nd isotopic systems in the global sedimentary systems. *Earth Planet. Sci. Lett.* **168,** 79–99.

von Blanckenburg F. and Igel H. (1999) Lateral mixing and advection of reactive isotope tracers in ocean basins: Observations and mechanisms. *Earth Planet. Sci. Lett.* **169,** 113–128.

Warren B. A. (1983) Why is no deep water formed in the North Pacific? *J. Mar. Res.* **41,** 327–347.

Weber E. T., Owen R. M., Dickens G. R., Halliday A. N., Jones C. E., and Rea D. K. (1996) Quantitative resolution of eolian continental crustal material and volcanic detritus in North Pacific surface sediment. *Paleoceanography* **11**(1), 115–127.

White W. M. and Patchett J. (1984) Hf-Nd-Sr isotopes and incompatible element abundances in island ars: Implications for magma origins and crust-mantle evolution. *Earth Planet. Sci. Lett.* **67,** 167–185.

White W. M., Patchett J., and Ben Othman D. (1986) Hf isotope ratios of marine sediments and Mn nodules: Evidence for a mantle source of Hf in seawater. *Earth Planet. Sci. Lett.* **79,** 46–54.

Wijffels S. E., Toole J. M., Bryden H. L., Fine R. A., Jenkins W. J., and Bullister J. L. (1996) The water masses and circulation at 10°N in the Pacific. *Deep-Sea Res. I* **43**(4), 501–544.

Zhang J., Amakawa H., and Nozaki Y. (1994) The comparative behaviors of Yttrium and Lanthanides in the seawater of the North Pacific. *Geophys. Res. Lett.* **21**(24), 2677–2680.